J. Fluid Mech. (2020), *vol.* 900, A27. © The Author(s), 2020.
Published by Cambridge University Press
doi:10.1017/jfm.2020.495

Modelling Lagrangian velocity and acceleration in turbulent flows as infinitely differentiable stochastic processes

Bianca Viggiano[1,2], Jan Friedrich[1], Romain Volk[1], Mickael Bourgoin[1], Raúl Bayoán Cal[1,2] and Laurent Chevillard[1,†]

[1]Laboratoire de Physique, Univ Lyon, Ens de Lyon, Univ Claude Bernard, CNRS, 46 allée d'Italie, F-69342 Lyon, France

[2]Department of Mechanical and Materials Engineering, Portland State University, Portland, OR 97201, USA

(Received 20 September 2019; revised 23 April 2020; accepted 15 June 2020)

We develop a stochastic model for Lagrangian velocity as it is observed in experimental and numerical fully developed turbulent flows. We define it as the unique statistically stationary solution of a causal dynamics, given by a stochastic differential equation. In comparison with previously proposed stochastic models, the obtained process is infinitely differentiable at a given finite Reynolds number, and its second-order statistical properties converge to those of an Ornstein–Uhlenbeck process in the infinite Reynolds number limit. In this limit, it exhibits furthermore intermittent scaling properties, as they can be quantified using higher-order statistics. To achieve this, we begin with generalizing the two-layered embedded stochastic process of Sawford (*Phys. Fluids* A, vol. 3 (6), 1991, pp. 1577–1586) by considering an infinite number of layers. We then study, both theoretically and numerically, the convergence towards a smooth (i.e. infinitely differentiable) Gaussian process. To include intermittent corrections, we follow similar considerations as for the multifractal random walk of Bacry *et al.* (*Phys. Rev.* E, vol. 64, 2001, 026103). We derive in an exact manner the statistical properties of this process, and compare them with those estimated from Lagrangian trajectories extracted from numerically simulated turbulent flows. Key predictions of the multifractal formalism regarding the acceleration correlation function and high-order structure functions are also derived. Through these predictions, we understand phenomenologically peculiar behaviours of the fluctuations in the dissipative range, that are not reproduced by our stochastic process. The proposed theoretical method regarding the modelling of infinitely differentiability opens the route to the full stochastic modelling of velocity, including the peculiar action of viscosity on the very fine scales.

Key words: homogeneous turbulence, isotropic turbulence, turbulence theory

1. Introduction

Stochastic modelling of Lagrangian velocity and acceleration has a long history in the literature of turbulent flows (see Pope 1990; Pope & Chen 1990; Sawford 1991; Borgas &

† Email address for correspondence: laurent.chevillard@ens-lyon.fr

Sawford 1994; Wilson & Sawford 1996; Pope 2002; Beck 2003; Friedrich 2003; Mordant *et al.* 2003; Reynolds 2003; Sawford *et al.* 2003; Reynolds *et al.* 2005; Lamorgese *et al.* 2007; Minier, Chibbaro & Pope 2014, and references therein). Typical modelling approaches consist of proposing a random process in time for the velocity $v(t)$ of a tracer particle advected by a turbulent flow begins with reproducing the expected behaviour given by the standard phenomenology of turbulence. At very large Reynolds number, in a sustained, statistically stationary, turbulent flow of characteristic large integral length scale L, (i) Lagrangian velocity itself is a statistically stationary process of finite variance $\langle v^2\rangle = \sigma^2$ and is correlated over a large time scale $T \propto L/\sigma$, (ii) it is non-differentiable (i.e. rough) such that the velocity increment variance $\langle(\delta_\tau v)^2\rangle$, where $\delta_\tau v(t) = v(t+\tau) - v(t)$, is proportional to τ as the scale τ becomes smaller. This is the standard dimensional picture of Lagrangian turbulence at infinite Reynolds numbers (Monin & Yaglom 1971; Tennekes & Lumley 1972). Nonetheless, at a finite Reynolds number, let us stress that v is regularized at small scales by viscosity, and an appropriate modelling must produce differentiable kinematic quantities.

From a stochastic point of view, we could wonder whether a random process $v(t)$ with $t \in \mathbb{R}$, and its respective dynamics ensuring causality could be built with the capability of reproducing these aforementioned statistical properties. More precisely, rephrased in terms inherited from the mathematics of stochastic differential equations, we would like to define such a process $v(t)$ as the solution of an evolution equation forced by a random force. Henceforth, we will attribute the causality property to a given random process $v(t)$ if its infinitesimal increment $\mathrm{d}v(t) \equiv v(t+\mathrm{d}t) - v(t)$ over $\mathrm{d}t$ is governed by the history of $v(t)$ (or any functionals of it) up to time t, and additional non-anticipative filtering of the Wiener process (see for instance the textbook of Nualart (2000)). In this context, the simplest linear and Markovian stochastic evolution is given by the so-called Ornstein–Uhlenbeck (OU) process that reads

$$\mathrm{d}v(t) = -\frac{1}{T}v(t)\,\mathrm{d}t + \sqrt{\frac{2\sigma^2}{T}}W(\mathrm{d}t), \tag{1.1}$$

where $W(\mathrm{d}t)$ is an instance of the increment over $\mathrm{d}t$ of a Gaussian Wiener process. It can be understood in a heuristic way as a collection of independent realizations of a zero-average Gaussian random variable of variance $\mathrm{d}t$ (i.e. a white noise). The statistical properties of the unique solution $v(t)$ of this evolution (1.1) are precisely reviewed in § 2.1. We can nonetheless notice that since v is defined as a linear operation on a Gaussian random force, it is necessarily Gaussian itself, and is indeed consistent with a finite-variance process $\langle v^2\rangle = \sigma^2$ and the linear behaviour of its respective second-order structure function $\langle(\delta_\tau v)^2\rangle$ with τ representing the time delay (see the discussion in § 2.1 and (2.7)).

Going beyond this simple phenomenology, and its respective stochastic modelling, we would like to include finite Reynolds number effects, and in particular acquire a stochastic description of the related acceleration process $a(t) = \mathrm{d}v(t)/\mathrm{d}t$. Notice that the stochastic evolution of $v(t)$ using a OU process (1.1) is typical of a non-differentiable process, and thus fails to reproduce proper statistical behaviours for a. To do so, we have to replace the white noise term $W(\mathrm{d}t)$ entering in (1.1) by a finite-variance random force, correlated over a non-vanishing time scale τ_η, that eventually depends on viscosity, known as the dissipative Kolmogorov time scale. If we furthermore assume that this random force is itself defined as the solution of an OU process of characteristic time scale τ_η, we recover the two-layered embedded stochastic model of Sawford (1991). We review its statistical properties in § 2.2.1. This model is appealing since it incorporates, in a simple way, the additional necessary time scale τ_η implied by the finite value of viscosity, or equivalently, the finite value of the Reynolds number. Both velocity and acceleration are statistically stationary and of finite variance in this framework, and the predicted acceleration correlation function reproduces in a consistent way the fact that it has to cross zero in the vicinity of τ_η, before decaying towards 0 over T. Nonetheless, whereas the model gives an appropriate description of the velocity correlation function in both the inertial and dissipative ranges, further comparisons with numerical data (see respective discussions in Sawford (1991), Lamorgese *et al.* (2007)) underlined its limitations regarding the behaviour of the acceleration correlation function in the dissipative range, i.e. for time lags smaller than this zero-crossing time scale.

Obviously, in the model of Sawford (1991), whereas velocity is differentiable, leading to a finite-variance acceleration process, it is not twice differentiable: the obtained acceleration process is not a differentiable random function. This observation has strong implications on the shape of the acceleration correlation function. In particular, in the dissipative range, as observed in numerical data for both velocity and acceleration, and expected from the physical point of view when viscosity is finite, correlation functions of differentiable random functions are parabolic (or smoother) in the vicinity of the origin, whereas the predicted acceleration correlation function of Sawford (1991) behaves linearly. Modelling Lagrangian velocity by a two-layered embedded OU process, hence, appears to be too simplistic to reproduce the correlation structure of acceleration in the dissipative range.

For this reason, we found it relevant and original to develop and generalize the model of Sawford (1991) in order to provide a meaning and answer to the following question: can we construct a causal stochastic process which is infinitely differentiable at a given finite Reynolds number, or equivalently at a given finite dissipative time scale τ_η, consistent with the standard aforementioned phenomenology of turbulence in the inertial range (i.e. for scales $\tau_\eta \ll \tau \ll T$), and that converges towards an OU process (1.1) at infinite Reynolds numbers (or equivalently as $\tau_\eta \to 0$)? We indeed develop in §§ 2.2.2 and 2.3 such a process. It is obtained as the generalization of the framework of Sawford (1991) to n layers, the first layer corresponding to a Langevin process of characteristic time scale T, and then $n-1$ layers corresponding to the dynamics of the random forcing term given by Langevin processes of characteristic time scale τ_η. Infinite differentiability is attained while iterating this procedure for an infinite number of layers $n \to \infty$, while properly normalizing the small time scale τ_η by a factor $\sqrt{n}$ to ensure a non-trivial convergence, as is rigorously done in § 2.3. We eventually end up with an infinitely differentiable causal random process, which is Gaussian, and derive in an exact manner its statistical properties (listed in Proposition A.2). We furthermore propose a first numerical illustration of this process in § 2.4, through the simulation of a time series of velocity and its respective acceleration, and comparison with theoretical expressions.

As mentioned, since its dynamics is made of embedded linear operations on a Gaussian white noise, it is itself Gaussian. Such a Gaussian framework, in particular for acceleration, is at odds with experimental and numerical investigations of Lagrangian turbulence (see Yeung & Pope 1989; Voth, Satyanarayan & Bodenschatz 1998; La Porta *et al.* 2001; Mordant *et al.* 2001, 2002, 2003; Chevillard *et al.* 2003; Friedrich 2003; Biferale *et al.* 2004; Toschi & Bodenschatz 2009; Pinton & Sawford 2012; Bentkamp, Lalescu & Wilczek 2019, and references therein). As correctly predicted by Borgas (1993), the observed level of intermittency in the Lagrangian framework is found much higher than in the Eulerian framework (Frisch 1995).

To reproduce these highly non-Gaussian features of Lagrangian turbulence, we propose then to extend the construction of the current infinitely differentiable process to include the intermittent, i.e. multifractal, nature of the fluctuations. To do so, we first revisit the construction of the so-called multifractal random walk of Bacry, Delour & Muzy (2001) that was shown in Mordant *et al.* (2002) to reproduce several key aspects of Lagrangian intermittency. Compared with previously published investigations, we include, in an original way, the notion of causality in this non-Gaussian random walk. We design a stochastic evolution for the probabilistic model of the intermittency phenomenon (i.e. the multiplicative chaos) in § 3.1. We then proceed with deriving in a rigorous way its statistical properties, and list them in Proposition A.3 and § 3.1. Finite Reynolds number effects, and the implied infinite differentiability, are then included in a similar fashion as in the first part of the article. Developments on this intermittent and infinitely differentiable process are proposed in § 3.2, and we highlight its statistical properties in Propositions A.4–A.6. As we explain in § 3.1, including intermittency implies the introduction of a non-Markovian step, that is necessary to reproduce the high level of roughness (that we define precisely) implied by the multifractal structure of the trajectories. This, then, asks for the design of a novel numerical algorithm able to simulate in an efficient way its time series. We propose in § 3.3.1 such an algorithm in which efficiency is based on its formulation in the Fourier space, allowing optimal consideration given its non-Markovian nature. Simulations of the time series of velocity and acceleration are proposed in § 3.3.2, where we compare the numerical estimation of their statistical properties with our theoretical predictions.

Section 4 is devoted to the comparison of the statistical properties of the infinitely differentiable multifractal process with trajectories extracted from direct numerical simulations (DNSs) of the Navier–Stokes equations (see details on the database in § 4.1). To make this comparison transparent and reproducible, we explain in § 4.4.2 the chosen procedure to calibrate the model parameters τ_η and T, and their link to the physical parameters of the DNS data. Overall, we find good agreement between the statistical properties of the DNS data, and of those predicted by our theoretical approach. We nonetheless underline some discrepancies on the flatness of velocity increments in the dissipative range: As detailed in § 4.5, the model does not reproduce the observed rapid increase of the flatness in the dissipative range, a behaviour which is known to be related to the very peculiar differential action of viscosity on the final damping of the singularities developed by the flow.

This motivates the final investigation that we propose in § 5 where we derive the corresponding predictions as they are obtained from the multifractal formalism (Frisch 1995). As far as we know, this has never been done for the acceleration correlation function, and we take special care to quantify precisely the respective prediction for the Reynolds number dependence of acceleration variance (see § 5.2.3). Compared with the previous approach, aimed at building a stochastic process as the solution of a causal dynamical evolution, the multifractal formalism is not as complete from a probabilistic point of view: we do not obtain the time series of velocity and acceleration, but only model some of their statistical properties (i.e. their high-order structure functions). Once again the calibration procedure is detailed (§ 5.3) and proceeded by the comparison with DNS data. We observe also an excellent agreement between predictions and estimations based on DNS data. In particular, which is our initial motivation, multifractal formalism, and its modelling of a fluctuating dissipative time scale, is able to reproduce this rapid increase of the flatness in the dissipative range.

We gather conclusions and perspectives in § 6.

2. Ordinary and embedded Ornstein–Uhlenbeck processes as statistically stationary models for Lagrangian velocity and acceleration

2.1. *Ordinary single-layered Ornstein–Uhlenbeck process*

Standard arguments developed in turbulence phenomenology (Tennekes & Lumley 1972) lead to the consideration of, as a stochastic model for velocity of Lagrangian tracers, the OU process. In particular, such a process reaches a statistically stationary regime in which variance is finite and exponentially correlated. Let us denote such a process by $v_1(t)$, and define it as the unique stationary solution of the following stochastic differential equation, also called Langevin equation,

$$\mathrm{d}v_1(t) = -\frac{1}{T}v_1(t)\,\mathrm{d}t + \sqrt{q}W(\mathrm{d}t), \tag{2.1}$$

where T is the turbulence (large) turnover time, $W(t)$ is a Wiener process and $W(\mathrm{d}t)$ its infinitesimal increment over $\mathrm{d}t$ (i.e. independent instances of a Gaussian random variable, zero average and of variance $\mathrm{d}t$). It obeys the following rule of calculation (cf. Nualart 2000): any appropriate deterministic functions f and g, which follow particular integrability conditions such that,

$$\left\langle \int_{\mathcal{A}} f(t)W(\mathrm{d}t) \right\rangle = 0, \tag{2.2}$$

and

$$\left\langle \int_{\mathcal{A}} f(t)W(\mathrm{d}t) \int_{\mathcal{B}} g(t)W(\mathrm{d}t) \right\rangle = \int_{\mathcal{A}\cap\mathcal{B}} f(t)g(t)\,\mathrm{d}t, \tag{2.3}$$

where $\langle\cdot\rangle$ stands for ensemble average, and $\mathcal{A}\cap\mathcal{B}$ is the intersection of the two ensembles $\mathcal{A}$ and $\mathcal{B}$.

The unique statistically stationary solution of the stochastic differential equation (SDE) provided in (2.1) can be written conveniently as

$$v_1(t) = \sqrt{q}\int_{-\infty}^{t} \mathrm{e}^{-(t-t')/T}W(\mathrm{d}t'). \tag{2.4}$$

Since v_1 is defined as a linear operation on the Gaussian white noise $W(\mathrm{d}t)$, it is Gaussian itself. Following the rules given in (2.2) and (2.3), it is thus fully characterized by its average and correlation function. In particular, v_1 is a zero-average process, i.e. $\langle v_1\rangle = 0$, and is correlated as

$$\mathcal{C}_{v_1}(t_1-t_2) \equiv \langle v_1(t_1)v_1(t_2)\rangle = q\int_{-\infty}^{min(t_1,t_2)} \exp(-(t_1+t_2-2t)/T)\,\mathrm{d}t = \frac{qT}{2}\mathrm{e}^{-|t_1-t_2|/T}. \tag{2.5}$$

Notice that v_1 is a finite-variance process $\langle v_1^2\rangle = qT/2$ (consider the value of the correlation function (2.5) at equal times, $t_1=t_2$), and behaves at small scales as a Brownian motion, as is required by the dimensional arguments developed in the standard phenomenology of turbulence at infinite Reynolds number (Tennekes & Lumley 1972).

To see this, define the velocity increment as

$$\delta_\tau v_1(t) \equiv v_1(t+\tau) - v_1(t), \tag{2.6}$$

and notice that

$$\left\langle (\delta_\tau v_1(t))^2 \right\rangle = 2\left[\left\langle v_1^2 \right\rangle - \mathcal{C}_{v_1}(\tau)\right] \underset{\tau\to 0}{\sim} q|\tau|. \tag{2.7}$$

The scaling behaviour given in (2.7) is typical of non-differentiable processes. Hence, the respective acceleration process $a_1(t) \equiv \mathrm{d}v_1/\mathrm{d}t$ is ill-defined (actually it is a random distribution). To circumvent this pathological behaviour, Sawford (1991) has proposed introducing the dissipative Kolmogorov time scale τ_η, which will be discussed in the following section.

2.2. *Embedded Ornstein–Uhlenbeck processes*

2.2.1. *Two layers: the Sawford model*

Here, we follow the approach developed by Sawford (1991). We consider the following embedded OU process $v_2(t)$:

$$\frac{\mathrm{d}v_2}{\mathrm{d}t} = -\frac{1}{T} v_2(t) + f_1(t), \tag{2.8}$$

where $f_1(t)$ in an external random force that obeys itself an ordinary OU process, as discussed in § 2.1, but exponentially correlated over the small time scale τ_η. It is thus defined as the unique solution of the following SDE

$$\mathrm{d}f_1(t) = -\frac{1}{\tau_\eta} f_1(t)\,\mathrm{d}t + \sqrt{q}W(\mathrm{d}t). \tag{2.9}$$

Hence, it is a zero-average Gaussian process, and its correlation function is given by

$$\mathcal{C}_{f_1}(\tau) \equiv \langle f_1(t) f_1(t+\tau)\rangle = \frac{q\tau_\eta}{2}\mathrm{e}^{-|\tau|/\tau_\eta}. \tag{2.10}$$

The unique statistically stationary solution of (2.8) is once again given by

$$v_2(t) = \int_{-\infty}^{t} \mathrm{e}^{-(t-t')/T} f_1(t')\,\mathrm{d}t',$$

showing that v_2 is a zero-average Gaussian process, and correlated as

$$\mathcal{C}_{v_2}(\tau) \equiv \langle v_2(t) v_2(t+\tau)\rangle = \int_{-\infty}^{t}\int_{-\infty}^{t+\tau} \exp(-(2t+\tau-t_1-t_2)/T)\mathcal{C}_{f_1}(t_1-t_2)\,\mathrm{d}t_1\,\mathrm{d}t_2. \tag{2.11}$$

Assuming without loss of generality $\tau \geq 0$ (recall that the correlation function of a statistically stationary process is an even function of its argument), splitting the integral entering in (2.11) over the dummy variable t_2 into the two sets $[-\infty, t]$ and $[t, t+\tau]$, and performing the remaining explicit double integral, we obtain the following expression:

$$\mathcal{C}_{v_2}(\tau) = \frac{q\tau_\eta^2 T^2}{2(T^2-\tau_\eta^2)}\left[T\mathrm{e}^{-|\tau|/T} - \tau_\eta \mathrm{e}^{-|\tau|/\tau_\eta}\right], \tag{2.12}$$

which is in agreement with the formula given by Sawford (1991).

The respective acceleration process $a_2(t) \equiv \mathrm{d}v_2(t)/\mathrm{d}t$, obtained from (2.8), is accordingly a zero-average Gaussian process, and its correlation function is given by

$$\begin{aligned} \mathcal{C}_{a_2}(\tau) &\equiv \langle a_2(t) a_2(t+\tau)\rangle \\ &= -\frac{\mathrm{d}^2}{\mathrm{d}\tau^2}\langle v_2(t)v_2(t+\tau)\rangle = \frac{q\tau_\eta^2 T^2}{2(T^2-\tau_\eta^2)}\left[-\frac{1}{T}\mathrm{e}^{-|\tau|/T} + \frac{1}{\tau_\eta}\mathrm{e}^{-|\tau|/\tau_\eta}\right]. \end{aligned} \tag{2.13}$$

Notice that the function $\mathcal{C}_{v_2}$ (2.12) is indeed twice differentiable at the origin, contrary to the function $\mathcal{C}_{v_1}$ (2.5), such that a_2 has finite variance given by $\mathcal{C}_{a_2}(0)$ (2.13).

2.2.2. *Generalization to n layers*

By iterating the aforementioned procedure, we can consider similarly n additional layers instead of a single one, as proposed in the embedded Ornstein–Uhlenbeck process (2.8) by Sawford. Here, acceleration is a well-defined random process and so are the velocity derivatives of order n. Once again, these additional layers will eventually be modelled as OU processes. A similar type of procedure has been adopted in Arratia, Cabana & Cabana (2014) in a different context. The obtained embedded structure is defined using a set of n coupled stochastic ordinary differential equations (ODEs), with $n \geq 2$, that reads

$$\frac{\mathrm{d}v_n}{\mathrm{d}t} = -\frac{1}{T}v_n(t) + f_{n-1}(t), \tag{2.14}$$

$$\frac{\mathrm{d}f_{n-1}}{\mathrm{d}t} = -\frac{1}{\tau_\eta}f_{n-1}(t) + f_{n-2}(t), \tag{2.15}$$

$$\cdots \tag{2.16}$$

$$\frac{\mathrm{d}f_2}{\mathrm{d}t} = -\frac{1}{\tau_\eta}f_2(t) + f_1(t), \tag{2.17}$$

$$\mathrm{d}f_1 = -\frac{1}{\tau_\eta}f_1(t)\,\mathrm{d}t + \sqrt{q_{(n)}}W(\mathrm{d}t). \tag{2.18}$$

The remaining free parameter $q_{(n)}$ can be eventually chosen such that

$$\langle v_n^2\rangle = \sigma^2, \tag{2.19}$$

independently of τ_η and/or the number of layers n, as is required by the standard phenomenology of Lagrangian turbulence (Tennekes & Lumley 1972).

We present in Proposition A.1 the explicit computation of the correlation functions of velocity v_n and the respective acceleration a_n in the statistically stationary regime, obtained from the set of (2.14)–(2.18) as $t \to \infty$. Their expressions are especially simple in the spectral domain, and read, considering $n \geq 2$ to ensure that acceleration is a well-defined process,

$$\mathcal{C}_{v_n}(\tau) = q_{(n)}\int_{\mathbb{R}} \mathrm{e}^{2\mathrm{i}\pi\omega\tau}\frac{T^2}{1+4\pi^2T^2\omega^2}\left[\frac{\tau_\eta^2}{1+4\pi^2\tau_\eta^2\omega^2}\right]^{n-1}\mathrm{d}\omega, \tag{2.20}$$

and

$$\mathcal{C}_{a_n}(\tau) = q_{(n)}\int_{\mathbb{R}} 4\pi^2\omega^2\mathrm{e}^{2\mathrm{i}\pi\omega\tau}\frac{T^2}{1+4\pi^2T^2\omega^2}\left[\frac{\tau_\eta^2}{1+4\pi^2\tau_\eta^2\omega^2}\right]^{n-1}\mathrm{d}\omega, \tag{2.21}$$

where the multiplicative factor $q_{(n)}$ (defined in (A 6)) enforces the prescribed value of velocity variance (2.19). Let us notice that taking $n = 2$ layers, the respective correlation of the process v_2 coincides with the one proposed in Sawford (1991), as recalled in § 2.2.1.

It is interesting to consider the limiting process v or a when the number of layers n goes towards infinity from a physical point of view, which would give an example of a causal infinitely differentiable process, if such a process exists. It is indeed possible to show rigorously that the correlation function of v_n (2.20) loses its dependence on the time scale τ. We then have $\mathcal{C}_{v_n}(\tau) \to \sigma^2$ for any $\tau \geq 0$ as $n \to \infty$. Thus, asymptotically, the limiting process does not decorrelate, which is at odds with the expected behaviour. We will see in the following § 2.3 that by considering the re-scaled dissipative time scale $\tau_\eta/\sqrt{n-1}$ instead of τ_η, the system of equations will converge towards a proper process with an appropriate correlation function as $n \to \infty$.

2.3. *Towards an infinitely differentiable causal process*

Consider the following system of embedded differential equations:

$$\frac{\mathrm{d}v_n}{\mathrm{d}t} = -\frac{1}{T} v_n(t) + f_{n-1}(t), \tag{2.22}$$

$$\frac{\mathrm{d}f_{n-1}}{\mathrm{d}t} = -\frac{\sqrt{n-1}}{\tau_\eta} f_{n-1}(t) + f_{n-2}(t), \tag{2.23}$$

$$\cdots \tag{2.24}$$

$$\frac{\mathrm{d}f_2}{\mathrm{d}t} = -\frac{\sqrt{n-1}}{\tau_\eta} f_2(t) + f_1(t), \tag{2.25}$$

$$\mathrm{d}f_1 = -\frac{\sqrt{n-1}}{\tau_\eta} f_1(t)\,\mathrm{d}t + \sqrt{\alpha_n}\, W(\mathrm{d}t), \tag{2.26}$$

with

$$\alpha_n = \left(\frac{n-1}{\tau_\eta^2}\right)^{n-1} \frac{2\sigma^2 \mathrm{e}^{-\tau_\eta^2/T^2}}{T \operatorname{erfc}\left(\tau_\eta/T\right)}, \tag{2.27}$$

where we have introduced the error function $\operatorname{erf}(t) = (2/\sqrt{\pi}) \int_0^t \mathrm{e}^{-s^2}\,\mathrm{d}s$, and its respective complementary $\operatorname{erfc}(t) = 1 - \operatorname{erf}(t)$. The chosen white noise weight α_n (2.27) ensures that the variance of the limiting process v is finite with $\langle v^2 \rangle = \sigma^2$.

We summarize and derive in appendix A (see Proposition A.2) the statistical properties of the unique statistically stationary solution of the set of embedded differential (2.22)–(2.26). In particular, the velocity correlation function now reads

$$\mathcal{C}_{v_n}(\tau) = \frac{2\sigma^2 \mathrm{e}^{-\tau_\eta^2/T^2}}{T \operatorname{erfc}\left(\tau_\eta/T\right)} \int_{\mathbb{R}} \mathrm{e}^{2\mathrm{i}\pi\omega\tau} \frac{T^2}{1 + 4\pi^2 T^2 \omega^2} \left[\frac{1}{1 + \dfrac{4\pi^2 \tau_\eta^2 \omega^2}{n-1}}\right]^{n-1} \mathrm{d}\omega. \tag{2.28}$$

Whereas the function provided in (2.20) does not converge towards a correlation function of a well-behaved stochastic process as the number of layers goes to infinity, (2.28) does. In other words, through iteration of the set of embedded differential equations, (2.22)–(2.26), over an infinite number of layers $n \to \infty$, we obtain an infinitely differentiable and causal Gaussian process, in which the velocity correlation function reads, in the stationary regime,

$$\mathcal{C}_v(\tau) = \sigma^2 \frac{\mathrm{e}^{-|\tau|/T}}{2\mathrm{erfc}(\tau_\eta/T)} \left[1 + \mathrm{erf}\left(\frac{|\tau|}{2\tau_\eta} - \frac{\tau_\eta}{T} \right) + \mathrm{e}^{2|\tau|/T}\mathrm{erfc}\left(\frac{|\tau|}{2\tau_\eta} + \frac{\tau_\eta}{T} \right) \right]. \quad (2.29)$$

Let us notice that indeed $\mathcal{C}_v(0) = \langle v^2 \rangle = \sigma^2$. Furthermore, taking the second derivatives of (2.29) and multiplying by the factor $-1/2$, we obtain the respective acceleration correlation function

$$\mathcal{C}_a(\tau) = \frac{\sigma^2}{2T^2\mathrm{erfc}(\tau_\eta/T)} \left[\frac{2T}{\tau_\eta \sqrt{\pi}} \exp\left(-\left(\frac{\tau^2}{4\tau_\eta^2} + \frac{\tau_\eta^2}{T^2} \right) \right) - \mathrm{e}^{-|\tau|/T} \left(1 + \mathrm{erf}\left(\frac{|\tau|}{2\tau_\eta} - \frac{\tau_\eta}{T} \right) \right) \right.$$
$$\left. - \mathrm{e}^{|\tau|/T}\mathrm{erfc}\left(\frac{|\tau|}{2\tau_\eta} + \frac{\tau_\eta}{T} \right) \right]. \quad (2.30)$$

2.4. *A first numerical illustration*

A first numerical illustration is proposed to observe numerically how the statistical characteristics of the Gaussian process v_n, typically its correlation function and the one of the associated acceleration for a given set of values of the parameters τ_η and T go towards the limiting process v (and given in Proposition A.2) as the number of layers n increases. This limiting process v, being Gaussian and of zero average, is completely characterized by its correlation function (2.29) in the statistically stationary regime, and could be obtained as a linear operation on the white Gaussian noise. Performing such a simulation is possible, although a causal kernel would need to be found such that the correlation function is consistent with (2.29). Although interesting, this is not a simple task and this perspective is kept for future investigations. Furthermore, in subsequent numerical simulations, the convergence towards the statistically steady state while solving the transient regime is observed. For these reasons, the set of stochastic differential equations (2.22)–(2.26) for a given finite number of layers n will be solved, and thus give a numerical estimation of the process v_n and its statistical properties.

We perform a numerical simulation of the set of (2.22) to (2.26) using $n = 9$ layers, and for $\tau_\eta = T/10$. Choose, for instance, $T = 1$, which is equivalent to dimensionalized time scales in units of T. Time integration is performed with a simple Euler discretization scheme. The choice for $\mathrm{d}t$ is dictated by the smallest time scale of the system; here, $\tau_\eta/\sqrt{n-1}$. Presently for $n = 9$, we found the value $\mathrm{d}t = \tau_\eta/100$ small enough to guarantee the appropriate behaviour. We take $\sigma^2 = 1$, and the respective weight α_9 of the white noise is given in (2.27). Trajectories are then integrated over $10^4 T$ and results are shown in figure 1. We could have chosen to perform a simulation using more layers, although the simulation gets heavier, and as we will see, the statistical properties of the obtained process are observed very close to the asymptotic ones (as $n \to \infty$). Also, recall that the white noise weight α_{n+1} (2.27) increases as n^n, so from a numerical point of view, if n is chosen large, it may introduce additional rounding errors related to the double-precision floating-point format.

We display first in figure 1(a) an instance of the obtained processes $v_9(t)$ and its derivatives $a_9(t)$, over $5T$ after numerically integrating the (2.22)–(2.26). As claimed in Proposition A.2, the process v_9 (which correlation function is given in (2.28)) is 8-times differentiable. Its first derivative $a_9(t)$ is consequently 7-times differentiable; resulting in

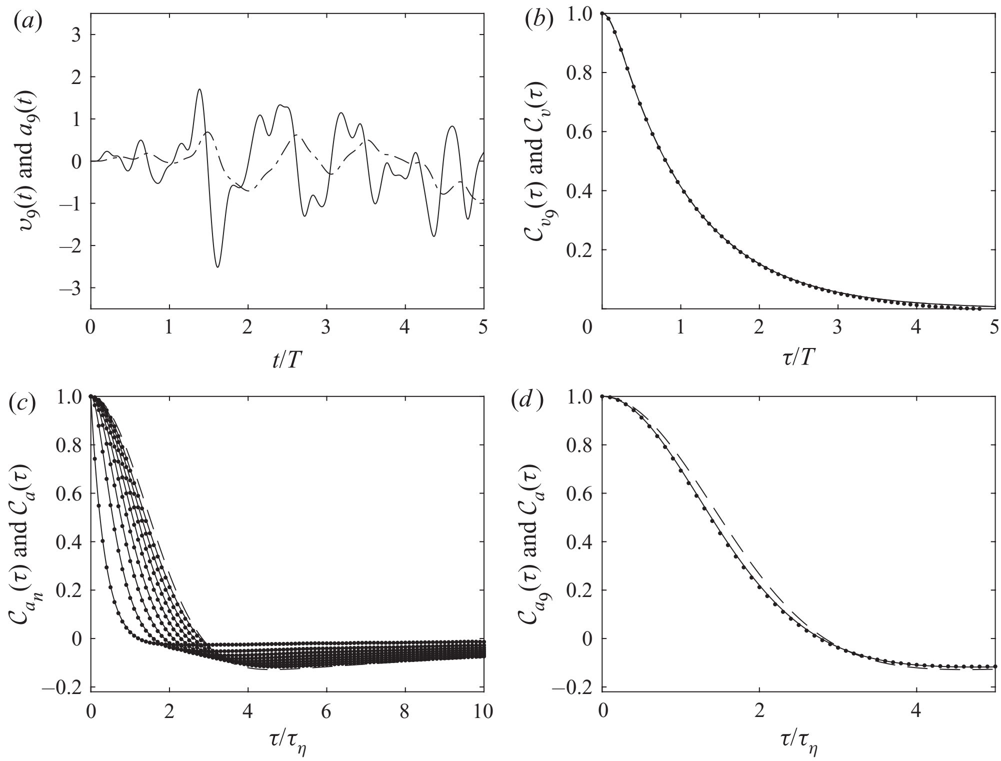

FIGURE 1. Numerical simulation of the set of (2.22)–(2.26) using $n = 9$ layers, for $\tau_\eta = T/10$ and $\sigma^2 = 1$ (see text). (*a*) Typical time series of the obtained processes $v_9(t)$ (dashed line) and $a_9(t)$ (solid line), as a function of time t. (*b*) Respective velocity correlation functions $\mathcal{C}_{v_9}$, estimated from numerical simulations (dots), theoretically derived from (2.28) (solid line), and the correlation function of the asymptotic process $\mathcal{C}_v$, of which the expression is provided in (2.29). (*c*) Acceleration correlation functions $\mathcal{C}_{a_n}$ using n layers, n ranging from 2 to 9 (from left to right), using $\sigma^2 = 1$ and $\alpha_n = \alpha_9$ (2.27). Numerical estimations from time series are displayed with dots, respective theoretical expressions from (2.28) are represented with solid lines, and the asymptotic correlation function $\mathcal{C}_a$ (2.30) is shown with a dashed line. For the sake of clarity, all curves are normalized by their values at the origin (i.e. the respective variances). (*d*) Similar plot as in (*c*), but only the layer $n = 9$ is displayed, over a shorter range of time lag τ.

a smooth profile correlated over τ_η. We could have performed a similar simulation using additional layers, although its estimated correlation functions of velocity and acceleration will eventually be close to the asymptotic ones of v (and provided in Proposition A.2).

In figure 1(*b*), we present three curves corresponding to (i) the estimated correlation function $\mathcal{C}_{v_9}$ (dots), (ii) its theoretical expression (solid line), obtained when performing the integral entering in (2.28) using a symbolic calculation software, and (iii) the asymptotic correlation function $\mathcal{C}_v$ given in (2.29) (dashed line). The profiles collapse, making it difficult to distinguish between these three curves. The velocity correlation functions $\mathcal{C}_{v_n}$ depend weakly on n (not shown). This can be understood easily since the dependence on n is only really crucial at the dissipative scales; scales that are solely highlighted by a small scale quantity such as acceleration.

In this context, we present in figure 1(*c*) the corresponding estimated and theoretical curves $\mathcal{C}_{a_n}$ for n ranging from 2 to 9 to observe and quantify the convergence of the acceleration correlation function towards its asymptotic regime. Recall that $\mathcal{C}_{a_2}$ corresponds to the prediction of Sawford (1991) (see (2.13)), which is characteristic of the correlation function of a non-differentiable process ($\mathcal{C}_{a_2}$ is not twice differentiable at the origin). A perfect agreement between the numerical estimation based on random time series, and the theoretical expressions is observed and also derivable from (2.28). As the number of layers n increases, the acceleration correlation functions become more and more curved at the origin, guaranteeing finite variance of higher-order derivatives. We superpose on this figure the associated asymptotic correlation function $\mathcal{C}_a$ using a dashed line. Its explicit expression is given in (2.30); $\mathcal{C}_{a_9}$ is indeed very close to $\mathcal{C}_a$, as shown in figure 1(*d*). This shows that considering $n = 9$ layers is enough to reproduce the statistical behaviours of the asymptotic process, at least for velocity and acceleration, which are our main concern.

3. An infinitely differentiable causal process, asymptotically multifractal in the infinite Reynolds number limit

We now elaborate on the system proposed in (2.22)–(2.26) in order to include intermittent, i.e. multifractal, corrections. We have to introduce more elaborate probabilistic objects to do so in the spirit of the multifractal random walk (Bacry *et al.* 2001), applied to the Lagrangian context by Mordant *et al.* (2002, 2003). Recall that the zero-average process $v(t)$, obtained as the limit when $n \to \infty$ of the causal system defining v_n ((2.22)–(2.26)), is Gaussian, thus fully characterized by its correlation function (given in Proposition A.2). To go beyond this Gaussian framework, where linear operations on a Gaussian white noise $W(\mathrm{d}t)$ are involved, we will consider in the sequel a nonlinear operation while exponentiating a Gaussian field $X(t)$. Such a logarithmic correlation structure guarantees multifractal behaviours (specified later). The so-obtained random field is '$\mathrm{e}^{\gamma X}$', where γ is a free parameter of the theory that encodes the level of intermittency. This can be seen as a continuous and stationary version of the discrete cascade models developed in turbulence theory (see Meneveau & Sreenivasan 1987; Benzi *et al.* 1993; Frisch 1995; Arneodo, Bacry & Muzy 1998 and references therein) and is known in the mathematical literature as a multiplicative chaos (Rhodes & Vargas 2014). For recent applications of such a random distribution to the stochastic modelling of Eulerian velocity fields, see for instance Pereira, Garban & Chevillard (2016) and Chevillard *et al.* (2019). The purpose of this section is to generalize such a probabilistic approach to a causal context, and to include finite Reynolds number effects that guarantee differentiability below the Kolmogorov time scale τ_η.

3.1. *A causal multifractal random walk*

Let us here review the stochastic modelling of the Lagrangian velocity proposed by Mordant *et al.* (2002, 2003), which is based on the multifractal process of Bacry *et al.* (2001). This process can be considered as an OU process (2.1) forced by a non-Gaussian uncorrelated random noise, and is called the multifractal random walk (MRW). Its dynamics reads

$$\mathrm{d}u_{1,\epsilon}(t) = -\frac{1}{T}u_{1,\epsilon}(t)\,\mathrm{d}t + \sqrt{q}\exp(\gamma X_{1,\epsilon}(t) - \gamma^2\langle X_{1,\epsilon}^2\rangle)W(\mathrm{d}t), \tag{3.1}$$

where a new random field $X_{1,\epsilon}$ is introduced. This random field is Gaussian, zero average and taken independent of the white noise instance $W(\mathrm{d}t)$, and is thus fully characterized by its correlation function. To reproduce intermittent corrections, as they have been observed in Lagrangian turbulence (see Yeung & Pope 1989; Voth *et al.* 1998; La Porta *et al.* 2001; Mordant *et al.* 2001, 2002, 2003; Chevillard *et al.* 2003; Biferale *et al.* 2004; Toschi & Bodenschatz 2009; Pinton & Sawford 2012; Bentkamp *et al.* 2019, and references therein), we demand the Gaussian field $X_{1,\epsilon}$ to be logarithmically correlated (Bacry *et al.* 2001). Such a correlation structure implies in particular that the variance of $X_{1,\epsilon}$ diverges as $\epsilon \to 0$, making it difficult to give a proper mathematical meaning to such a field. This divergence is even amplified when considering its exponential, as is proposed in (3.1). Instead, we rely on an approximation procedure, at a given (small) parameter ϵ, that will eventually play, loosely speaking, the role of the small time scale τ_η of turbulence. Such a logarithmic correlation structure has to be truncated over the large time scale T in order to ensure a finite variance. These truncations are well understood from a mathematical perspective (Rhodes & Vargas 2014), and a proper limit as $\epsilon \to 0$ leads to a well-defined, canonical, random distribution.

Nonetheless, nothing is said in Bacry *et al.* (2001) about causality. Causal representations of multifractal random fields have been previously made by Schmitt & Marsan (2001) and Bacry & Muzy (2003), yet these propositions are not defined as solutions of some stochastic evolutions. In order to include this important physical constraint, we define the field $X_{1,\epsilon}$ as the unique statistically stationary solution of a stochastic differential equation, that will eventually be consistent with both truncations over the time scales ϵ and T, and a logarithmic behaviour in between. Being Gaussian, and independent of the white noise $W(\mathrm{d}t)$ entering in (3.1), such dynamics has to be defined as a linear operation on an independent instance of the Gaussian white noise, call it $\widetilde{W}(\mathrm{d}t)$, such that $\langle W(\mathrm{d}t)\widetilde{W}(\mathrm{d}t')\rangle = 0$ at any time t and t'. In this context, such a linear stochastic evolution has been proposed by Chevillard (2017) and Pereira, Moriconi & Chevillard (2018), and reads

$$\mathrm{d}X_{1,\epsilon}(t) = -\frac{1}{T}X_{1,\epsilon}(t)\,\mathrm{d}t - \frac{1}{2}\int_{-\infty}^{t} [t-s+\epsilon]^{-3/2}\,\widetilde{W}(\mathrm{d}s)\,\mathrm{d}t + \epsilon^{-1/2}\widetilde{W}(\mathrm{d}t). \tag{3.2}$$

It can be seen as a fractional Ornstein–Uhlenbeck process of vanishing Hurst exponent (Chevillard 2017; Pereira *et al.* 2018). Remark also that the underlying integration over the past with a rapidly decreasing kernel that enters in the dynamics of $X_{1,\epsilon}$ (3.2) implies that we are dealing with non-Markovian processes. A precise and comprehensive characterization of the statistical properties of the fields $X_{1,\epsilon}$ and its asymptotical log-correlated version $X_1 \equiv \lim_{\epsilon\to 0} X_{1,\epsilon}$ can be found in Proposition A.3.

Let us focus on the statistical properties of the MRW that now includes a causal definition for the field X_1. We will work as much as possible, for the sake of presentation, in the asymptotic regime where we have taken the limit $\epsilon \to 0$. We keep in mind that the pointwise limit of such a process $u_1(t) = \lim_{\epsilon\to 0} u_{1,\epsilon}(t)$, where $u_{1,\epsilon}(t)$ is the unique statistically stationary solution of the SDE given in (3.1), is not straightforward to acquire, since the random field $\exp(\gamma X_{1,\epsilon}(t) - \gamma^2\langle X_{1,\epsilon}^2\rangle)$ becomes distributional in this limit (Rhodes & Vargas 2014). We will thus be mainly concerned with statistical quantities of the asymptotic random process u_1, but will perform standard calculations using the classical field $u_{1,\epsilon}(t)$ if necessary and convenient. Because we want to quantify the intermittent corrections implied by the this random distribution, we propose to compute the structure functions of the aforementioned stochastic model. Define thus the velocity increment as

$$\delta_\tau u_{1,\epsilon}(t) = u_{1,\epsilon}(t+\tau) - u_{1,\epsilon}(t). \tag{3.3}$$

Accordingly, define the respective asymptotic structure functions as

$$\mathcal{S}_{u_1,m}(\tau) = \lim_{\epsilon\to 0}\left\langle \left(u_{1,\epsilon}(t+\tau) - u_{1,\epsilon}(t)\right)^m\right\rangle. \tag{3.4}$$

In the following, we focus on the scaling properties of the structure functions of the causal MRW u_1. As a general remark, let us recall that the log-correlated field X_1 and the underlying white noise W entering in the dynamics of $u_{1,\epsilon}$ are taken independently. This implies that all odd-order structure functions vanish, namely $\mathcal{S}_{u_1,2m+1} = 0$ with $m \in \mathbb{N}$. Regarding the second-order structure function, it is the same as the one obtained from the OU process v_1 (2.1), and given by

$$\mathcal{S}_{u_1,2}(\tau) = \mathcal{S}_{v_1,2}(\tau) = qT\left[1 - \mathrm{e}^{-\frac{|\tau|}{T}}\right] \underset{\tau\to 0^+}{\sim} q\tau. \tag{3.5}$$

On the contrary, the fourth-order structure function is impacted by intermittency, and we get, under the condition $4\gamma^2 < 1$,

$$\mathcal{S}_{u_1,4}(\tau) \underset{\tau\to 0}{\sim} \frac{3}{1-6\gamma^2+8\gamma^4} q^2\tau^2\left(\frac{\tau}{T}\right)^{-4\gamma^2} \mathrm{e}^{4\gamma^2 c(0)}, \tag{3.6}$$

where the constant $c(0)$ is given in (A 18). More generally, it is then possible to obtain an estimation of the $(2m)$th-order structure functions that reads, for $2m(m-1)\gamma^2 < 1$,

$$\mathcal{S}_{u_1,2m}(\tau) \underset{\tau\to 0}{\propto} q^m\tau^m\left(\frac{\tau}{T}\right)^{-2m(m-1)\gamma^2}, \tag{3.7}$$

indicating that the causal MRW exhibits a log-normal spectrum. We gather all the proofs of these propositions in appendix B.

3.2. *An infinitely differentiable causal multifractal random walk*

Our proposition is herein made of a causal stochastic process representative of the statistical behaviour of Lagrangian velocity in homogeneous and isotropic turbulent flows at a given finite Reynolds number (equivalently for a finite ratio τ_η/T). We are demanding a statistically stationary process, correlated over a large time scale T, that is infinitely differentiable (giving meaning to the respective acceleration process), acquiring rough and intermittent behaviours as the small time scale τ_η goes to zero, i.e. in the infinite Reynolds number limit.

Assume $n \geq 2$ and consider the following system of embedded differential equations

$$\frac{\mathrm{d}u_{n,\epsilon}}{\mathrm{d}t} = -\frac{1}{T}u_{n,\epsilon}(t) + \exp\left(\gamma X_{n,\epsilon}(t) - \frac{\gamma^2}{2}\langle X_{n,\epsilon}^2\rangle\right) f_{n-1}(t), \tag{3.8}$$

$$\frac{\mathrm{d}f_{n-1}}{\mathrm{d}t} = -\frac{\sqrt{n-1}}{\tau_\eta} f_{n-1}(t) + f_{n-2}(t), \tag{3.9}$$

$$\cdots \tag{3.10}$$

$$\frac{\mathrm{d}f_2}{\mathrm{d}t} = -\frac{\sqrt{n-1}}{\tau_\eta} f_2(t) + f_1(t), \tag{3.11}$$

$$\mathrm{d}f_1 = -\frac{\sqrt{n-1}}{\tau_\eta} f_1(t)\,\mathrm{d}t + \sqrt{\beta_n}\, W(\mathrm{d}t), \tag{3.12}$$

with

$$\beta_n = \left(\frac{n-1}{\tau_\eta^2}\right)^{n-1} \frac{\sigma^2\sqrt{4\pi\tau_\eta^2}}{T\displaystyle\int_0^\infty \mathrm{e}^{-\frac{h}{T}}\mathrm{e}^{-h^2/(4\tau_\eta^2)}\mathrm{e}^{\gamma^2 \mathcal{C}_X(h)}\,\mathrm{d}h}. \tag{3.13}$$

In the system above, the causal process $X_{n,\epsilon}$ obeys the set of stochastic differential equations

$$\frac{\mathrm{d}X_{n,\epsilon}}{\mathrm{d}t} = -\frac{1}{T}X_{n,\epsilon}(t) + \sqrt{\tilde{\beta}_n}\tilde{f}_{n-1,\epsilon}(t), \tag{3.14}$$

$$\frac{\mathrm{d}\tilde{f}_{n-1,\epsilon}}{\mathrm{d}t} = -\frac{\sqrt{n-1}}{\tau_\eta}\tilde{f}_{n-1,\epsilon}(t) + \tilde{f}_{n-2,\epsilon}(t), \tag{3.15}$$

$$\cdots \tag{3.16}$$

$$\frac{\mathrm{d}\tilde{f}_{2,\epsilon}}{\mathrm{d}t} = -\frac{\sqrt{n-1}}{\tau_\eta}\tilde{f}_{2,\epsilon}(t) + \tilde{f}_{1,\epsilon}(t), \tag{3.17}$$

$$\mathrm{d}\tilde{f}_{1,\epsilon} = -\frac{\sqrt{n-1}}{\tau_\eta}\tilde{f}_{1,\epsilon}(t)\,\mathrm{d}t - \frac{1}{2}\int_{-\infty}^{t}[t-s+\epsilon]^{-3/2}\,\widetilde{W}(\mathrm{d}s)\,\mathrm{d}t + \epsilon^{-1/2}\widetilde{W}(\mathrm{d}t), \tag{3.18}$$

with

$$\tilde{\beta}_n = \left(\frac{n-1}{\tau_\eta^2}\right)^{n-1}. \tag{3.19}$$

where W and $\widetilde{W}$ are two independent copies of the Wiener process.

Similar to the Gaussian infinitely differentiable process v established in the first part, we show in the following Proposition A.5 that the process u, obtained once the procedure depicted in the set of embedded differential equations ((3.8)–(3.12)) is iterated an infinite number of times $n \to \infty$, and when the small parameter ϵ goes to zero, converges to a well-defined limit. Once again, the choice made for the white noise weight β_n (3.13) ensures that the variance of the limiting process u is finite with $\langle u^2\rangle = \sigma^2$. Its precise value will become evident when we compute the correlation function $\mathcal{C}_f(\tau) = \langle f(t)f(t+\tau)\rangle$ of the force f when $n \to \infty$ (see (A 29)).

Similarly, the precise choice for the coefficient $\tilde{\beta}_n$ (3.19) entering in the dynamics of $X_{n,\epsilon}$ (3.14) is dictated by the necessity that, in an asymptotic way, when both $\epsilon \to 0$ and $\tau_\eta \to 0$, and for any number of layers n, X_n becomes logarithmically correlated in an appropriate manner. As far as the process $X_{n,\epsilon}$ is concerned, these limits can be taken in an arbitrary way since they commute. The small parameters ϵ and τ_η have a similar physical interpretation, they mimic finite Reynolds number effects. We define them *a priori* as separate entities and seek for limits independently for the sake of generality. More precisely, ϵ is taken to be finite to make sense of the dynamics of $\tilde{f}_{1,\epsilon}$ as it is proposed in (3.18). Remark finally that the multiplicative chaos entering into the dynamics of $u_{n,\epsilon}$ (3.8) is renormalized by a smaller constant $\exp((\gamma^2/2)\langle X_{n,\epsilon}^2\rangle)$ than in its non-differentiable version $u_{1,\epsilon}$ (3.1), where there typically exists a larger normalization constant $\exp(\gamma^2\langle X_{n,\epsilon}^2\rangle)$. It is related to the finite correlation of the of the term f_{n-1} entering in (3.8), contrary to the dynamics proposed in (3.1), where a white noise $W(\mathrm{d}t)$ enters.

As a general remark, notice that the dynamics depicted by the set of embedded differential equations ((3.8)–(3.12)) coincides with the dynamics of the Gaussian process

v_n ((2.22)–(2.26)) when we consider the particular value $\gamma = 0$. In other words, the non-intermittent limit of the process $u_{n,\epsilon}$ is Gaussian, and coincides with the process v_n of § 2.3.

Before establishing the statistical behaviour of the asymptotic process u, let us first focus on the statistical properties of $X_{n,\epsilon}$ that we gather and derive in Proposition A.4. Keeping in mind that whatever the ordering of the limits $n \to \infty$ and $\epsilon \to 0$, the correlation function of $X_{n,\epsilon}$ converges towards a well-defined function $\mathcal{C}_X(\tau)$ (A 21), the value of which at the origin diverges logarithmically with τ_η as $\tau_\eta \to 0$ (A 24). Actually, in this limit of infinite Reynolds numbers, $\mathcal{C}_X(\tau)$ converges towards $\mathcal{C}_{X_1}(\tau)$ (A 25), as expected.

We now proceed with the covariance structure of the limiting process u. We summarize and demonstrate in Proposition A.5 the main second-order statistical properties of velocity u and acceleration a. We first derive the exact velocity correlation function $\mathcal{C}_u(\tau)$ in the joint commuting limit $\epsilon \to 0$ and $n \to \infty$ (A 28). This shows that, whereas $\mathcal{C}_u(\tau)$ depends weakly on intermittent corrections in the dissipative range, it loses this property as $\tau_\eta/T \to 0$ and coincides with the correlation function of the OU process $\mathcal{C}_{v_1}(\tau)$ (A 30). Similarly, the acceleration correlation function $\mathcal{C}_a(\tau)$ can be derived (A 32). From there, we show that acceleration variance diverges as T/τ_η as the Reynolds number increases (A 34).

Let us remark that the proposed stochastic model of velocity, u, that we claim to be intermittent in a precise way and defined in Proposition A.6, predicts that, as far as the covariance of u is concerned, it is similar to an Ornstein–Uhlenbeck process at infinite Reynolds number, independently of any intermittency corrections. This is consistent with the standard phenomenology of Lagrangian turbulence. The predicted acceleration variance (A 34) does not exhibit either intermittent corrections: this precise behaviour of acceleration variance with respect to the Reynolds number is at odds with the extrapolations that can be made from numerical simulations (cf. Ishihara *et al.* (2007) and the discussion that we propose in § 5.3). We will see and develop in § 5 that the multifractal formalism allows the understanding of how the velocity correlation does not get impacted by intermittency at infinite Reynolds numbers, whereas the acceleration variance does.

Let us now present the intermittent, i.e. multifractal, properties of the velocity process u, as they can be seen on higher-order structure functions (see Proposition A.6). As shown previously, the correlations of u and the OU process v_1 coincide as $\tau_\eta \to 0$. The same goes for the second-order structure function (A 37). Whereas showing that the fourth-order structure function of u coincides with that of the causal MRW process u_1 as first $\epsilon \to 0$ and then $\tau_\eta \to 0$ is obvious (A 38), the reversed order of limits is more involved. We nonetheless propose an approximation procedure that confirms that u and u_1 possess the same intermittent properties (A 39). All statements and proofs can be found in Proposition A.6 and appendix C.

3.3. *A second numerical illustration*

3.3.1. *An efficient algorithm under the periodic approximation*

In this section we propose a numerical algorithm able to reproduce in a realistic and efficient fashion the statistical behaviour of the process u, which statistical properties are detailed in Propositions A.5 and A.6. As we have seen, the process u, contrary to the Gaussian process v of § 2.3, obeys a non-Markovian dynamics. More precisely, for the process $X(t)$ at a given time t, the limiting solution, as the number of layers n goes to infinity and the small parameter ϵ goes to 0, of the system of embedded stochastic differential equations (3.14)–(3.18), requires the knowledge of its entire past. It is thus tempting to use the discrete Fourier transform to solve its dynamics. We will incidentally generate periodic solutions of this non-Markovian dynamics. Since we will consider in the sequel very long trajectories, of order 10^5 times the largest time scale T of the process, all aliasing effects will be negligible. This periodic approximation is well justified. As argued in § 2.4, simulations of the limiting process with $n \to \infty$ require the causal factorization of covariance functions of underlying Gaussian components, a procedure which is not simple. Furthermore, the limit $\epsilon \to 0$ is also complicated to obtain from a numerical point of view, and therefore, we will perform simulations for a finite n number of layers, and for a finite $\epsilon > 0$.

Consider first an estimator for the discrete process $\widehat{X}_{n,\epsilon}[t]$ of the continuous solution $X_{n,\epsilon}(t)$ of the coupled system (3.14)–(3.18). Let us introduce the convolution product $*$, which is defined as, for any two functions g_1 and g_2,

$$(g_1 * g_2)(\tau) = \int_{\mathbb{R}} g_1(t) g_2(\tau - t)\, \mathrm{d}t,$$

with the corresponding shorthand notation,

$$g^{*n} = \underbrace{g * g * \cdots * g}_{n}.$$

In the statistically stationary regime, the continuous expression of the Gaussian process $X_{n,\epsilon}(t)$ reads

$$X_{n,\epsilon}(t) = \sqrt{\widetilde{\beta}_n} \left(g_T * g^{*(n-1)}_{\frac{\tau_\eta}{\sqrt{n-1}}} * \left(h_\epsilon + \epsilon^{-1/2}\delta\right) * \widetilde{W} \right)(t), \tag{3.20}$$

where the multiplicative factor $\widetilde{\beta}_n$ is given in (3.19), and recall that $g_\tau(t) = \mathrm{e}^{-t/\tau} 1_{t\geq 0}$. We also include $h_\epsilon(t) = -\frac{1}{2}(t+\epsilon)^{-3/2} 1_{t\geq 0}$ and $\delta(t)$ stands for the Dirac delta function.

Now in the discrete setting, call N the number of collocation points, T_{tot} the total length of the simulation and Δt the time step. As already mentioned, make sure that $T_{tot} = N\Delta t \gg T$ to prevent aliasing errors. In the aforementioned periodic framework, the discrete estimator $\widehat{X}_{n,\epsilon}[t]$ of the continuous solution $X_{n,\epsilon}(t)$ (3.20) reads

$$\widehat{X}_{n,\epsilon}[t] = \sqrt{\widetilde{\beta}_n} \mathrm{DFT}^{-1} \left(\mathrm{DFT}\,(g_T)\, \mathrm{DFT}^{n-1} \left(g_{\frac{\tau_\eta}{\sqrt{n-1}}} \right) \mathrm{DFT}_c\,(h_\epsilon)\, \mathrm{DFT}\left(\widetilde{W}\right) \right)[t] \times (\Delta t)^n, \tag{3.21}$$

where we have introduced the discrete Fourier transform (DFT). It also enters in the expression given in (3.21), properly discretizing and periodizing forms of the continuous functions $g_\tau(t)$ at various time scales τ and $h_\epsilon(t)$. Notice that in the continuous framework, $\int_{\mathbb{R}} h_\epsilon(t)\,\mathrm{d}t = -\epsilon^{-1/2}$ is the value at the origin of frequencies of the Fourier transform (FT) of h_ϵ, such that $\mathrm{FT}(h_\epsilon + \epsilon^{-1/2}\delta)(\omega) = \mathrm{FT}(h_\epsilon)(\omega) - \mathrm{FT}(h_\epsilon)(0)$. This justifies the shorthand notation $\mathrm{DFT}_c(h_\epsilon)[\omega] = \mathrm{DFT}(h_\epsilon)[\omega] - \mathrm{DFT}(h_\epsilon)[0]$ in (3.21). Finally, we have noted $\widetilde{W}[t]$ an instance of the white noise field, comprised of N independent Gaussian random variables of zero average and variance Δt. The $(\Delta t)^n$ factor originates from the convolution by the kernel $g_T(t)$ and $(n-1)$ convolutions by the kernel $g_{\tau_\eta/\sqrt{n-1}}$.

In a similar manner, the numerical, discretized and periodized estimator $\hat{u}_{n,\epsilon}$ of the continuous solution $u_{n,\epsilon}$ of the coupled system (3.8)–(3.12) in the statistically stationary regime, which reads

$$u_{n,\epsilon}(t) = \sqrt{\beta_n}\left(g_T * g^{*(n-1)}_{\frac{\tau_\eta}{\sqrt{n-1}}} * \left(\frac{e^{\gamma \widehat{X}_{n,\epsilon}}}{\exp\left(\frac{\gamma^2}{2}\langle \widehat{X}^2_{n,\epsilon}\rangle\right)} W\right)\right)(t), \tag{3.22}$$

can be written as

$$\hat{u}_{n,\epsilon}[t] = \sqrt{\beta_n}\mathrm{DFT}^{-1}\left(\mathrm{DFT}\,(g_T)\,\mathrm{DFT}^{n-1}\left(g_{\frac{\tau_\eta}{\sqrt{n-1}}}\right)\mathrm{DFT}\left(\frac{e^{\gamma \widehat{X}_{n,\epsilon}}}{\exp\left(\frac{\gamma^2}{2}\langle \widehat{X}^2_{n,\epsilon}\rangle\right)} W\right)\right)[t] \times (\Delta t)^{n-1}, \tag{3.23}$$

where β_n is provided in (3.13), and recall that the white noise W is independent of $\widetilde{W}$ that enters in (3.21). The fact that we multiply by $(\Delta t)^{n-1}$ the overall expression 3.23, instead of $(\Delta t)^n$ (as in (3.21)), originates from the white (i.e. distributional) nature of W, whereas $\widetilde{W}$ is already smoothed out by the kernel h_ϵ.

The time step Δt has to be chosen to be smaller than the smallest scale of motion, that is $\tau_\eta/\sqrt{n-1}$. Furthermore, we are interested in performing a realistic simulation of the limiting process u, obtained in the limit $\epsilon \to 0$, at a given finite τ_η. A convenient choice for ϵ is to take it proportional to Δt, such that both of them go to zero in the continuous limit. In subsequent simulations, we find it appropriate to choose

$$\Delta t = \frac{\tau_\eta}{200\sqrt{n-1}} \quad \text{and} \quad \epsilon = 5\Delta t. \tag{3.24a,b}$$

This choice gives numerical stability and a proper illustration of the exact statistical quantities provided in Propositions A.5 and A.6 for the range of investigated values of τ_η (see the following § 3.3.2). To prevent aliasing errors, we work with a large number of collocation points $N = 2^{32}$, such that $T_{tot} = N\Delta t$ is always much larger than T.

3.3.2. *Numerical results and comparisons with theoretical predictions*

Without loss of generality, we take $T = 1$. We numerically perform the (discrete) Fourier transforms as they are detailed in (3.21) and (3.23), using six values for T/τ_η, that is 10, 20, 50, 100, 200 and 500. Keeping in mind that τ_η is a fairly good representation of the Kolmogorov time scale, these values correspond to an extended range of Reynolds numbers. Choosing for Δt and ϵ the values depicted in (3.24*a*,*b*), working with $N = 2^{32}$ collocation points and $n = 9$ layers, we find in the worst scenario corresponding to the smallest τ_η a total time of simulation $T_{tot} = N\Delta t \approx 10^4 T$, preventing any aliasing effects. As will be precisely quantified when we discuss intermittent corrections, we find the particular value

$$\gamma^2 = 0.085, \tag{3.25}$$

representative of the level of intermittency seen in numerical simulations of the Navier–Stokes equations, consistent with previous estimations (see Mordant *et al.* 2002; Chevillard *et al.* 2003; Biferale *et al.* 2004; Chevillard *et al.* 2012 and references therein).

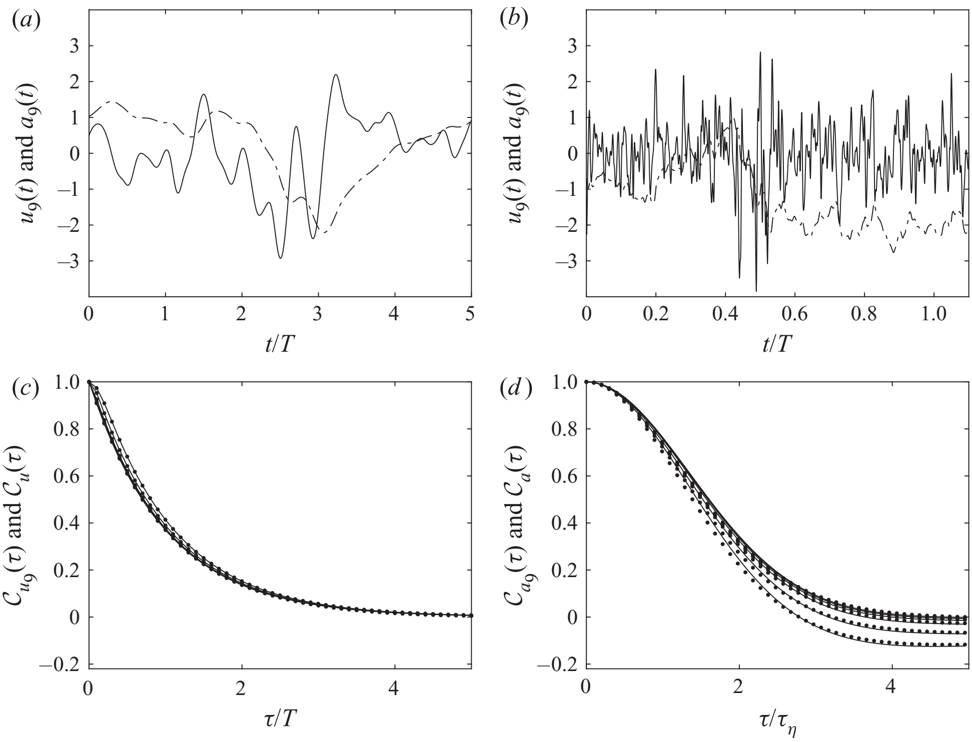

FIGURE 2. Numerical simulation, in a periodical fashion, of the set of (3.8)–(3.12) using $n = 9$ layers, for 6 values of τ_η, that is $T/\tau_\eta = 10$, 20, 50, 100, 200, 500 and $\sigma^2 = 1$. See the description of the algorithm in § 3.3.1, and the choice made for other parameters in § 3.3.2. (*a*) Typical time series of the obtained processes $u_9(t)$ (dashed line) and $a_9(t)$ (solid line), as a function of time t, for $T/\tau_\eta = 10$. For the sake of comparison, all time series are normalized by their standard deviation. (*b*) Similar time series as in (*a*), but for $T/\tau_\eta = 500$. (*c*) Respective velocity correlation functions $\mathcal{C}_{u_9}$ for the six different values of τ_η, estimated from numerical simulations (dots), compared with their asymptotic theoretical prediction $\mathcal{C}_u$ (A 28) (solid line). (*d*) Respective acceleration correlation functions $\mathcal{C}_{a_9}$ compared with the asymptotic correlation function $\mathcal{C}_a$ (A 32). For the sake of clarity, all curves are normalized by their values at the origin (i.e. the respective variances).

Forthcoming statistical quantities are averaged over three independent instances of these trajectories.

For the sake of clarity, we omit the hat on the simulated discrete version of $u_{9,\epsilon}$, and display in figure 2(*a*,*b*) two instances of this stochastic process for the largest $\tau_\eta = T/10$ (lowest Reynolds number) and the smallest $\tau_\eta = T/500$ (highest Reynolds number) ratios of the small over the large time scales. Velocity is represented using a dot-dashed line, whereas the respective acceleration with a solid line. All time series are divided by their respective standard deviation for the sake of comparison. In the low Reynolds number case (figure 2*a*), we observe that indeed velocity is correlated over t, whereas acceleration is correlated over a shorter time scale τ_η. In the highest Reynolds number case (figure 2*b*), we can definitely observe the scale decoupling between the large T and the small τ_η time scales. Also, notice that the statistics of acceleration are evidently non-Gaussian. This is a manifestation of the intermittency phenomenon, which is modelled by the multiplicative chaos that enters into the construction. These non-Gaussian fluctuations

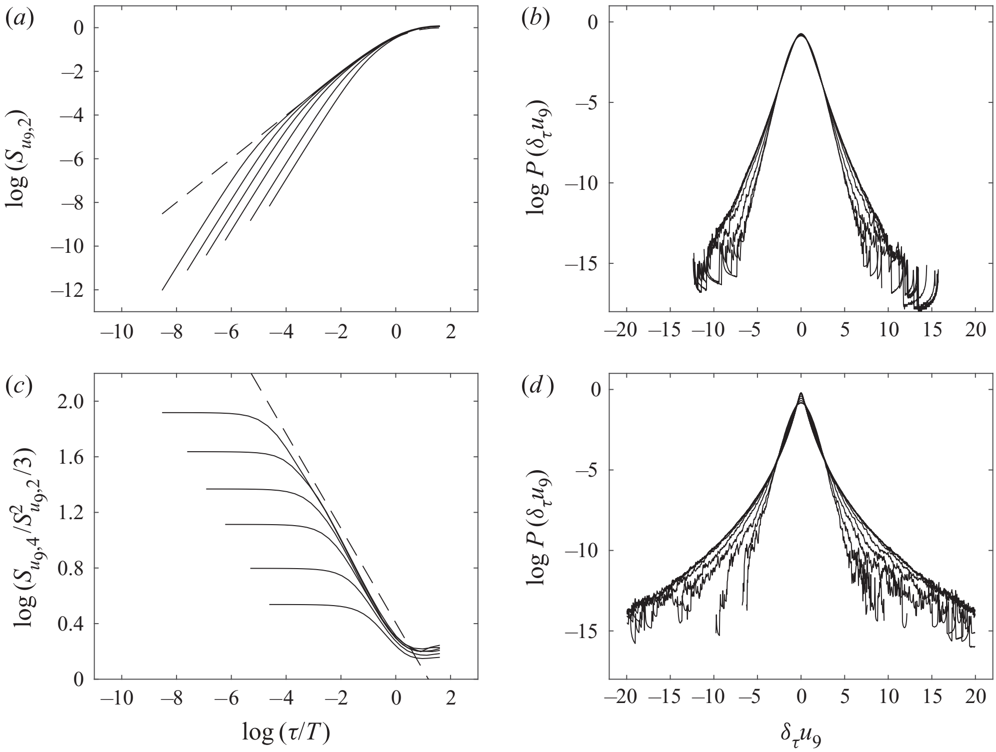

FIGURE 3. Illustration of the behaviour of higher-order statistics of the processes studied in figure 2. (*a*) Logarithmic representation of the second-order structure function, estimated from the times series of the six different values of τ_η (solid lines), and compared with their asymptotic prediction provided in (A 37) (dashed line). (*c*) Similar logarithmic process as in (*a*), but for the flatness of velocity increments. We superimpose the theoretical prediction based on (3.6) (see the devoted discussion in § 3.3.2). (*b*) Estimation of the probability density functions of velocity increments for scales logarithmically spanning the accessible range of scales displayed in (*a*,*c*), and for $\tau_\eta/T = 1/10$. (*d*) Similar plot as in (*b*) but for $\tau_\eta/T = 1/500$.

would be enhanced by a higher value of γ (data not shown) than the one chosen presently (3.25). We will come back to this point while discussing figure 3.

We present in figure 2 the velocity (*c*) and acceleration (*d*) correlation functions. Results from the numerical simulation of (3.21) and (3.23) for the six values of τ_η are displayed using dots; we superimpose the theoretical expressions provided in (A 28) and (A 32). Concerning the velocity correlations (figure 2*c*), we can notice the striking agreement between the numerical estimation based on time series of $u_{9,\epsilon}$ and the limiting theoretical expression (A 28), as was already observed in the Gaussian case (figure 1). Furthermore, as expected, the dependence on τ_η is very weak. This can be easily understood by realizing that the velocity is a large scale quantity, mostly governed by the physics taking place at T. In this regard, acceleration correlation functions will highlight the physics ruling phenomena which occur at τ_η and are displayed in figure 2(*d*). All curves are normalized by the respective value at the origin (i.e. the acceleration variance). The low Reynolds number case (largest τ_η) is easily recognizable; this is the curve going the most negative after the zero crossing. As τ_η decreases, $\mathcal{C}_a(\tau)$ is closer to 0. This is consistent with the constraint that the integral of this curve has to vanish, as a consequence of statistical stationarity.

Once again, the collapse of the numerically estimated $\mathcal{C}_{a_9}(\tau)$ (dots) onto the limiting theoretical expression given in (A 32) (solid line) is excellent.

Let us now focus on the precise quantification on the intermittency phenomenon. We display in figure 3(*a*,*c*) the behaviour across scales τ of the structure functions $\mathcal{S}_{u_{n,\epsilon},m} = \langle(\delta_\tau u_{n,\epsilon})^m\rangle$ of the simulated process $u_{n,\epsilon}$. We then compare them with our theoretical predictions (Proposition A.6) obtained in the asymptotic regime $n \to \infty$, $\epsilon \to 0$, $\tau_\eta \to 0$ and finally $\tau \to 0$ (limits are taken in this order).

We present in figure 3(*a*) the scaling behaviour of the second-order structure function $\mathcal{S}_{u_{9,\epsilon},2}(\tau) = \langle(\delta_\tau u_{9,\epsilon})^2\rangle$ (solid lines) for the 6 values of τ_η that we formerly detailed. Notice that, in this representation, $\mathcal{S}_{u_{9,\epsilon},2}(\tau)$ is normalized by $2\langle u_{9,\epsilon}^2\rangle$, such that it goes to unity at large arguments $\tau \gg T$. We recover at small scales $\tau \ll \tau_\eta$ the dissipative behaviour $\mathcal{S}_{u_{9,\epsilon},2}(\tau) \propto \tau^2$, which is a consequence of the differentiable nature of the process. In the inertial range $\tau_\eta \ll \tau \ll T$, as expected by our theoretical prediction (A 37), we get a behaviour similar to an OU process, that is $\mathcal{S}_{u_{9,\epsilon},2}(\tau) \propto \tau$. We superimpose using a dashed line the expected behaviour from an OU process, namely $S_{u_1,2}(\tau) = 2\langle u_1^2\rangle(1 - \mathrm{e}^{-|\tau|/T})$. We indeed observe that it describes with great accuracy the scaling behaviour of $\mathcal{S}_{u_{9,\epsilon},2}(\tau)$ in the inertial range and at larger scales. The second-order statistics of $u_{9,\epsilon}$ are well described by our asymptotic predictions in this range of scales. Similar conclusions were obtained while describing velocity correlation function in figure 2(*c*).

As mentioned in Proposition A.6, only fourth-order statistics and higher are impacted by intermittency. To check this, we represent in figure 3(*c*) the scaling behaviour of the flatness of velocity increments, that is $\mathcal{S}_{u_{9,\epsilon},4}/\mathcal{S}^2_{u_{9,\epsilon},2}$ (solid lines), for the 6 different values of τ_η, in a logarithmic fashion. As shown, flatnesses are normalized by 3, i.e. the value obtained for Gaussian processes. As we can observe, flatnesses are close to 3 at large scales $\tau \geq T$, and then increase in the inertial range as a power law, before saturating in the dissipative range $\tau \leq \tau_\eta$. This saturation is typical of differentiable processes: a Taylor series of increments makes the dependence on τ disappear. We superimpose on this plot, using a dashed line, the theoretical prediction that we made for MRW (3.6) without the unjustified additional free parameter. We indeed see that the power-law exponent is given by $-4\gamma^2$, and that the multiplicative constant is close to the one derived for the non-differentiable MRW (3.6). This theoretical prediction seems to be more and more representative of the intermittent properties of $u_{9,\epsilon}$ as τ_η gets smaller and smaller. This indicates that the constant $c_{\gamma,4}$ which is tedious to compute in an exact fashion (but easily accessible in the approximate framework developed in appendix C) for the infinitely differentiable MRW (A 39) is the same as in the non-differentiable case (3.6). This shows that the limits $\epsilon \to 0$ and $\tau_\eta \to 0$ commute at the fourth order too ((A 38) and (A 39)). This remains to be done on rigorous grounds.

Finally, to illustrate the intermittent behaviour of the process $u_{9,\epsilon}$, we display in figure 3(*b*,*d*) the probability density functions (PDFs) of velocity increments at various scales, from large to small: (*b*) $\tau_\eta/T = 1/10$ and (*d*) $\tau_\eta/T = 1/500$. We indeed observe the continuous shape deformation of these PDFs as the scale τ decreases in length, being Gaussian at large scales $\tau \geq T$, and strongly non-Gaussian in the dissipative range. In a manner consistent with the behaviour of the flatnesses (figure 3*c*), the acceleration PDF, obtained when $\tau \ll \tau_\eta$, is less and less Gaussian as τ_η diminishes in size.

4. Comparison with direct numerical simulations

4.1. *Description of the datasets*

We consider in this article two sets of data that have been made freely accessible to the public. We focus our attention on statistically homogeneous and isotropic numerical

Origin	Resolution	$\mathcal{R}_\lambda$	τ_K	T_L	Number of trajectories	dt	Duration
Turbase	512^3	185	0.0470	0.7736	126 720	4.10^{-3}	17.063 T_L
JHTDB	1024^3	418	0.0424	1.3003	32 768	2.10^{-3}	7.692 T_L

TABLE 1. Summary of relevant physical parameters of the two sets of DNS data. Resolution of the Eulerian fields, Taylor based Reynolds number $\mathcal{R}_\lambda$ and Kolmogorov dissipative time scale τ_K (4.2) are provided in relevant publications (see text). The Lagrangian integral time scale T_L is defined in (4.1) and is computed from our statistical estimation of the velocity correlation function.

flows obtained by solving the Navier–Stokes equations in a periodic box. Lagrangian trajectories are then extracted from the time evolution of the Eulerian fields while integrating the positions of tracer particles, initially distributed homogeneously in space. The first set concerns a direct numerical simulation (DNS) at a moderate Taylor based Reynolds number $\mathcal{R}_\lambda = 185$, referenced in Bec *et al.* (2006), Bec *et al.* (2011), which can be downloaded from https://turbase.cineca.it/. The second dataset concerns a higher Taylor based Reynolds number $\mathcal{R}_\lambda = 418$, hosted at Johns Hopkins Turbulence Database (JHTDB) (see http://turbulence.pha.jhu.edu). Details on this DNS and how to extract the Lagrangian trajectories can be found in Li *et al.* (2008) and Yu *et al.* (2012). Relevant parameters and specificities of these datasets and of the Lagrangian trajectories are given in table 1.

4.2. *Definition and estimation of the Lagrangian integral time scale*

Let us now make a connection between the present modelling approach, and its parameters, and numerical investigations. To do so, we have to consider quantities that can be extracted from DNS data, and show how to relate them to the free parameters entering in the definition of the stochastic process u, which are at a given Reynolds number τ_η, T and γ.

Call T_L the Lagrangian integral time scale, defined as the integral of the velocity correlation function, i.e.

$$T_L = \int_0^\infty \frac{\mathcal{C}_u(\tau)}{\mathcal{C}_u(0)}\,\mathrm{d}\tau, \tag{4.1}$$

where u stands for any Lagrangian velocity components extracted from DNS data, or the present stochastic model.

On the one hand, the definition of T_L (4.1) is appealing because it can be applied to and estimated from velocity time series coming indifferently from DNS or the model. On the other hand, it requires proper statistical convergence of the velocity correlation $\mathcal{C}_u(\tau)$ that is especially difficult to get from DNS at large time scales τ close to the velocity decorrelation time scale. This is even more true when considering experimental data (see a recent discussion on this by Huck, Machicoane & Volk (2019)) in which the duration of trajectories are usually shorter. Moreover, on the entire accessible statistical sample, made of tens (even one hundred in the moderate Reynolds number case) of thousands of trajectories for each of the three velocity components, we have observed a non-negligible level of anisotropy for both sets of data, the standard deviation of the variance of the three velocity components is of the order of 20 % of the average variance. We found this level of anisotropy surprising given the isotropic and periodic boundary conditions of the advecting flow. We are forced to reach the conclusion that, in both cases, trajectories are not long enough to guarantee statistical isotropy. This has consequences for the estimation of T_L. Nonetheless, and because we expect ultimately that the flow, and incidentally its Lagrangian trajectories, are isotropic, we average the velocity correlation function over the three components, keeping in mind that the lack of statistical convergence can imply a non-negligible error in the estimation of this large time scale. We gather our findings in table 1. Notice that this observed anisotropy on the velocity variance has weak impact on the acceleration correlation function once normalized by its value at the origin (data not shown). This can be understood by realizing that acceleration is governed by the small scales of the flow, and velocity by the large ones.

4.3. *Statistical analysis of the DNS datasets*

We display in figure 4(*a*,*c*) the numerical estimation of velocity and acceleration correlation functions based on the Lagrangian trajectories extracted from DNS, at moderate Reynolds number $\mathcal{R}_\lambda = 185$ (using open circles ○) and at high Reynolds number $\mathcal{R}_\lambda = 418$ (using open squares □). As $\mathcal{C}_u(\tau)$ is concerned (figure 4*a*), we normalize time lags τ by a large time scale T coming from the adopted calibration procedure of our model, and that we properly define in § 4.4.2. At this level of discussion, keep in mind that T is very close to T_L (4.1). Concerning $\mathcal{C}_a(\tau)$ (figure 4*c*), we normalize time lags τ by the Kolmogorov time scale τ_K that reads

$$\tau_K = \sqrt{\frac{\nu}{\langle\varepsilon\rangle}}, \tag{4.2}$$

where ν is the kinematic viscosity and $\langle\varepsilon\rangle$ the average viscous dissipation per unit of mass. Interestingly, we observe that, in this representation, where scales are normalized by τ_K, $\mathcal{C}_a(\tau)$ crosses zero at a Reynolds number independent time scale. Call such a scale τ_0, thus defined by $\mathcal{C}_a(\tau_0) = 0$. Indeed, this was already observed in numerical and laboratory flows (Yeung *et al.* 2007; Huck *et al.* 2019): the zero-crossing time scale of acceleration has a universal (i.e. Reynolds number independent) behaviour with respect to the Kolmogorov time scale τ_K (4.2), such that

$$\tau_0 \approx 2.2\,\tau_K, \tag{4.3}$$

in the range of investigated Kolmogorov time scales. In our case and to be more precise, we find $\tau_0 = 2.11\,\tau_K$ at $\mathcal{R}_\lambda = 185$, and $\tau_0 = 2.14\,\tau_K$ at $\mathcal{R}_\lambda = 418$, indeed very close to previous findings of Yeung *et al.* (2007) (4.3). In the sequel, we will use this fact to fully calibrate our model, in particular while relating its free parameter τ_η to the characteristics of the numerical flows. We will revisit this point in § 4.4.2.

Similarly, we display the scaling behaviour of the second-order structure function $\mathcal{S}_{u,2}$ (figure 4*b*) and of the flatness of the velocity increments (figure 4*d*). We can easily observe the three expected ranges of scales: the dissipative one with $\mathcal{S}_{u,2}(\tau) \propto \tau^2$, the inertial one with $\mathcal{S}_{u,2}(\tau) \propto \tau$ and the saturation towards $2\langle u^2\rangle$ at larger scales. Concerning the flatness, similar behaviour is observed, saturation at the Gaussian value 3 at large scales, and a power-law behaviour in the inertial range, reminiscent of the intermittency phenomenon. We furthermore observe a more rapid increase in the intermediate dissipative range, and then a Reynolds number dependent saturation towards the flatness of acceleration. This is a known effect of the fine structure of turbulence, linked to subtle differential action of the viscosity that depends on the local regularity of the velocity field (Chevillard *et al.* 2003; Chevillard, Castaing & Lévêque 2005; Chevillard *et al.* 2006; Arneodo *et al.* 2008; Benzi *et al.* 2010; Chevillard *et al.* 2012). This phenomenon is well reproduced by the phenomenology of the intermittency phenomenon developed in the framework of the

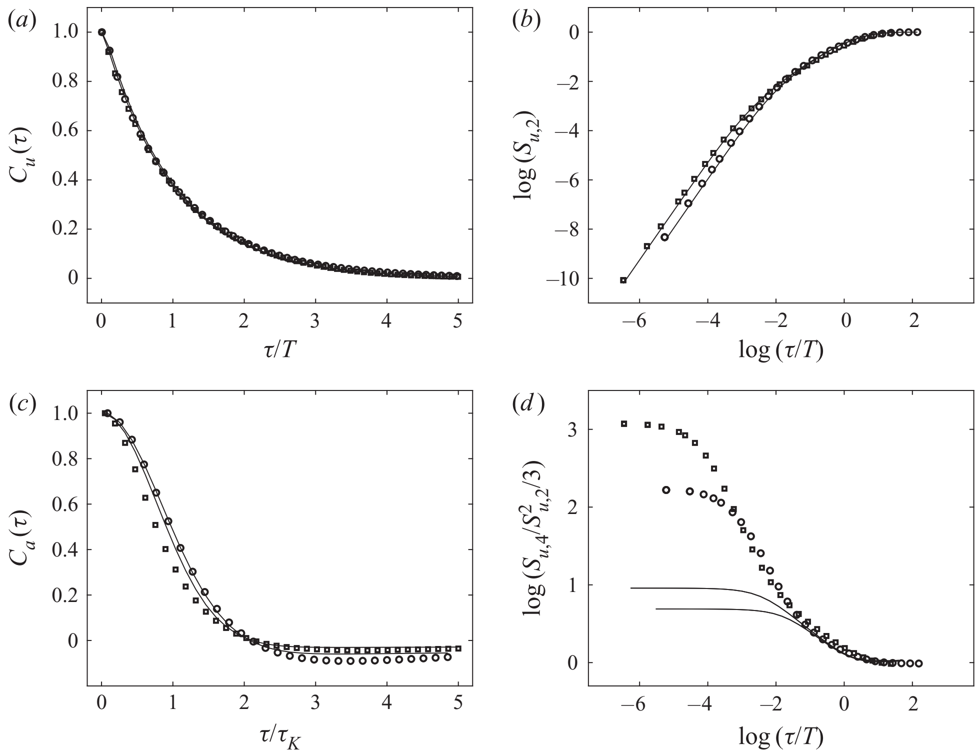

FIGURE 4. Comparison of DNS data with model predictions. (*a*) Estimation of the velocity correlation function from DNS data (using ○ for $\mathcal{R}_\lambda = 185$ and □ for $\mathcal{R}_\lambda = 418$. We superimpose theoretical predictions using (A 28), for the set of values of the parameters τ_η and T given by our calibration procedure presented in § 4.4.2, and for a prescribed value for γ (3.25). Time lags are normalized by the calibrated time scale T. (*b*) Same plot as in (*a*) but for the second-order structure function. (*c*) Similar plot as in (*a*,*b*) but for the acceleration correlation function, normalized by its value at the origin. Superimposed theoretical predictions are based on the exact expression (A 32). (*d*) Similar plot as in (*a*,*b*) but for the flatnesses of velocity increments. Theoretical prediction are obtained thanks to a numerical estimation of velocity time series of the model, in the spirit of § 3.3.2, with the values of the free parameters obtained from our calibration procedure presented in § 4.4.2 and for a prescribed value for γ (3.25).

multifractal formalism (Paladin & Vulpiani 1987; Frisch 1995). We will develop these ideas in § 5.

4.4. *Discussion on the Reynolds number dependence of the zero-crossing time scale of the acceleration correlation function*

4.4.1. *Model predictions of the zero-crossing time scales*

From previous developments, the present model, both for its Gaussian version v (Proposition A.2 and figure 1*d*) and for its intermittent generalization u (Proposition A.5 and figure 2*d*), predicts this aforementioned zero-crossing time scale τ_0 of the acceleration correlation function, as a function of its parameters τ_η and T. At this level of discussion, we neglect the influence of the intermittency parameter γ in this picture. Indeed, even if in the intermittent framework the parameter enters explicitly in the form of the correlation function (A 32), it has only a weak influence on its overall shape, even in the dissipative range (data not shown). Thus, given the low value of γ (3.25) that makes the predicted intermittent acceleration correlation function (A 32) indiscernible from its Gaussian approximation (2.30), we pursue further theoretical discussions neglecting these non-Gaussian effects. It is moreover convenient since in this case, $\mathcal{C}_a(\tau)$ has an explicit form (2.30), that makes its dependence present on τ_η and T.

Further inspection of the numerical results presented in figure 2(*d*) when τ_η is varying shows that this predicted zero-crossing time scale depends in a non-trivial way on τ_η. Actually, keeping only the leading terms entering in (2.30) as τ_η, we can observe that, asymptotically, this time scale behaves as

$$\tau_0 \underset{\tau_\eta \to 0}{\sim} 2\tau_\eta \sqrt{\log\left(\frac{T}{\sqrt{\pi}\tau_\eta}\right)}. \tag{4.4}$$

Taking into account the empirical fact that the zero-crossing time scale is proportional to the Kolmogorov time scale τ_K in a universal way (4.3), this shows that τ_η, up to logarithmic corrections, has the same Reynolds number dependence as τ_K, and thus can be considered as a dissipative time scale. Interestingly, for the process proposed by Sawford (§ 2.2.1), named here v_2, such a zero-crossing time scale can be exactly derived from (2.13). In this case, we obtain

$$\tau_0 = \tau_\eta \frac{\log(T/\tau_\eta)}{1 - \dfrac{\tau_\eta}{T}}.$$

The present prediction for τ_0 (4.4) made with an infinitely differentiable process can be seen as an improvement of the model by Sawford, since the parameter τ_η is closer to τ_K.

4.4.2. *The proposed calibration procedure of models parameters*

As explained in the preceding section, we can neglect in this discussion all possible intermittent effects, and work in a convenient way with the explicit second-order statistical properties of the Gaussian process v (Proposition A.2). To determine the free parameters of the model τ_η, given the characteristic scales of the DNS τ_K and T_L, we solve the nonlinear system of coupled equations

$$T_L = T \frac{\mathrm{e}^{-\tau_\eta^2/T^2}}{\operatorname{erfc}\left(\tau_\eta/T\right)}, \tag{4.5}$$

$$\mathcal{C}_a(\alpha\tau_K) = 0, \tag{4.6}$$

where the exact expression of T_L in (4.5) can be easily obtained from (A 8), the explicit expression of $\mathcal{C}_a$ is provided in (2.30), with α being equal to 2.11 at $\mathcal{R}_\lambda = 185$, and 2.14 at $\mathcal{R}_\lambda = 418$. This is our calibration procedure. Using a standard numerical solver of nonlinear equations and the values of (τ_K, T_L) provided in table 1, we look for the solution of the system of (4.5) and (4.6), and get $(\tau_\eta/\tau_K, T/T_L) = (0.6335, 0.9562)$ for $\mathcal{R}_\lambda = 185$, and $(0.5759, 0.9791)$ for $\mathcal{R}_\lambda = 418$.

4.5. *Comparison of model predictions with DNS data*

Having performed the calibration procedure depicted in § 4.4.2, and obtained the respective values for the free parameters τ_η and T, we compare the predictions of the present model with data. We represent theoretical second-order statistics in figure 4(*a*,*b*) using solid lines. We indeed observe an almost perfect collapse with the statistical estimations based on DNS data.

We focus now on the acceleration correlation function (figure 4*c*). At a moderate Reynolds number $\mathcal{R}_\lambda = 185$, we can see that the agreement is excellent in the dissipative range, i.e. for scales smaller that the zero-crossing time scale τ_0. We can also observe a slight disagreement above τ_0. This can be due to the lack of statistical convergence at large scales that induces an overestimation of the integral time scale T_L, as we discussed in § 4.2. Only a specially devoted DNS simulation, that would be run over several tens of large turnover time scales could show us whether the model predictions can be improved. At the current level of precision, we can consider that overall agreement with the second-order statistics is satisfactory at this Reynolds number. At a higher Reynolds number $\mathcal{R}_\lambda = 418$, further discrepancies can be seen in the dissipative range. This is very probably due to intermittency effects, that are negligible in the model, but not in the DNS. To see this more clearly, let us focus on the flatness of velocity increments.

We superimpose in figure 4(*d*) using solid lines the theoretical predictions that can be made from the model for flatnesses using the prescribed value γ^2 (3.25). To get these theoretical predictions, that are tedious to obtain in an analytical fashion, we perform additional numerical simulations of time series of the model, as is done in § 3.3.2, for the calibrated values of the parameters τ_η and T obtained in § 4.4.2. We observe a very good agreement in the inertial range, showing that the chosen value for the intermittency coefficient γ (3.25) is realistic of DNS. Unfortunately, as we already noticed in § 4.3, the model is unable to reproduce the rapid increase of intermittency in the dissipative range. To go further in this direction, we propose deriving the predictions of the multifractal formalism in the following § 5 concerning the behaviour of the flatnesses in this range of scales.

5. Predictions of the multifractal formalism regarding the acceleration correlation function

An alternative method of modelling the velocity and acceleration correlation functions consists in directly proposing their functional forms. We will thus construct models of the statistical behaviours of the velocity, that will take into account the various range of scales pointed out by the phenomenology of turbulence, namely the inertial and dissipative ranges (with additional intermittent corrections). Doing so, we will end up with an explicit form of the velocity correlation function, or equivalently the second-order structure function, without building up the underlying stochastic process. Compared with the previous construction of a stochastic process, from which we deduced its statistical behaviour, this approach appears only partial from a probabilistic point of view: we model the velocity correlation function (from which we deduce the acceleration correlation function) and higher-order moments of the velocity increments, but we do not characterize completely the velocity process itself. In this regard, the following probabilistic description is not complete, but will allow us, in particular, to understand in detail the rapid increase of the velocity increment flatness across the dissipative range, which is depicted in figure 4(*d*).

5.1. *The Batchelor parametrization of the second-order structure function*

We begin by proposing a simple model for the velocity correlation function, or equivalently a model of the second moment of the velocity increments. Concerning the

Eulerian framework, Batchelor (1951) proposed a simple form for the second-order structure function that includes the inertial behaviour $\langle(\delta_\ell u)^2\rangle \sim \ell^{2/3}$ and the dissipative behaviour $\langle(\delta_\ell u)^2\rangle \sim \ell^2$, with an additional polynomial interpolation relating these two behaviours across the Kolmogorov dissipative length scale (see for instance

Meneveau (1996) and Chevillard *et al.* (2006, 2012) for developments on this matter and references therein). A similar procedure can be adapted to the Lagrangian framework, that would include the respective inertial behaviour $\langle(\delta_\tau v)^2\rangle \sim \tau$ and the dissipative behaviour $\langle(\delta_\tau v)^2\rangle \sim \tau^2$, as was considered by Chevillard *et al.* (2003), Arneodo *et al.* (2008), Benzi *et al.* (2010) and Chevillard *et al.* (2012). Such a form reads, assuming $\tau \ll T$,

$$\mathcal{S}_2(\tau) = \langle(\delta_\tau v)^2\rangle = 2\sigma^2 \frac{\dfrac{\tau}{T}}{\left[1+\left(\dfrac{\tau}{\tau_\eta}\right)^{-\delta}\right]^{\frac{1}{\delta}}},$$

where τ_η is the typical dissipative (Kolmogorov) time scale, and $\sigma^2 = \langle v^2\rangle$. The additional free parameter δ governs the transition between the inertial and dissipative ranges of scales. For instance, as far as the Eulerian framework is concerned, the value $\delta = 2$ was chosen by Batchelor (1951). We will see that the value $\delta = 4$ will eventually reproduce in an appropriate manner the behaviour of the statistical quantities in the Lagrangian framework, as was chosen in Arneodo *et al.* (2008). At large scales, τ of the order of T and larger, we could think about multiplying the proposed form (5.1) by a cutoff function of characteristic time scale T, as was proposed in Bos *et al.* (2012). Such a procedure is necessary to ensure a smooth transition towards decorrelation. It is indeed required that $\mathcal{S}_2(\tau)$ goes to $2\sigma^2 = 2\langle v^2\rangle$ as $\tau \to \infty$. Incidentally, it will also make the integral of the velocity correlation function $C_v(\tau) \equiv \sigma^2 - \mathcal{S}_2(\tau)/2$ converge, as is required when assuming stationary statistics. Recall furthermore that we will be interested in looking at the second derivatives of $\mathcal{S}_2$ in order to describe the acceleration correlation, for which statistical stationarity implies that its integral over time lags τ vanishes. In this regard, multiplying by a cutoff function of characteristic time scale T turns out to be too schematic. Instead, we will be using the following *ad hoc* form, for any time lags $\tau \geq 0$,

$$\mathcal{S}_2(\tau) = \langle(\delta_\tau v)^2\rangle = 2\sigma^2 \frac{1-\mathrm{e}^{-\frac{\tau}{T}}}{\left[1+\left(\dfrac{\tau}{\tau_\eta}\right)^{-\delta}\right]^{\frac{1}{\delta}}}. \tag{5.1}$$

Correspondingly, the acceleration correlation function is given by (half) the second derivatives of (5.1), and we get, written in a convenient form,

$$\mathcal{C}_a(\tau) \equiv \frac{1}{2}\frac{\mathrm{d}^2\mathcal{S}_2(\tau)}{\mathrm{d}\tau^2}. \tag{5.2}$$

5.2. *Including intermittency corrections using the multifractal formalism*

The multifractal formalism (Frisch 1995) provides a convenient theoretical framework to generalize the approach of Batchelor (5.1) such that inclusion of intermittent corrections is possible, and consistent with high-order structure functions. Mostly developed for the

Eulerian framework, it has then been adapted to the Lagrangian framework by several authors and compared with great success with experimental and numerical data (see Borgas 1993; Chevillard *et al.* 2003; Biferale *et al.* 2004 and references therein). Here, we follow mainly the approach reviewed in Chevillard *et al.* (2012), where we furthermore include the smooth behaviour at large scales that was motivated in § 5.1.

5.2.1. *Second-order structure function and implied acceleration correlation using the language of the multifractal formalism*

In few words, arguments developed in this context concern the probabilistic modelling of the Lagrangian velocity increment, defined by $\delta_\tau v(t) = v(t+\tau) - v(t)$. In a similar spirit as the Batchelor parametrization of the second-order structure function (5.1), taking into account expected behaviours in the inertial and dissipative ranges, we get the following explicit expression for $\tau \geq 0$:

$$\mathcal{S}_2(\tau) = \langle (\delta_\tau v)^2 \rangle = 2\sigma^2 \int_{h_{min}}^{h_{max}} \frac{\left(1-\mathrm{e}^{-\frac{\tau}{T}}\right)^{2h}}{\left[1+\left(\dfrac{\tau}{\tau_\eta(h)}\right)^{-\delta}\right]^{\frac{2(1-h)}{\delta}}} \mathcal{P}_h^{(\tau)}(h)\,\mathrm{d}h, \tag{5.3}$$

which can be regarded as a generalization of the parametrization used in (5.1) to a non-unique exponent h that eventually fluctuates according to its probability density $\mathcal{P}_h^{(\tau)}$ at a given scale τ. Actually, we can recover exactly (5.1) while assuming a unique (non-fluctuating, i.e. deterministic) exponent $h = 1/2$, that corresponds to a distribution of density $\mathcal{P}_h^{(\tau)}$ equal to the Dirac delta function centred on this unique value 1/2. Remark also that we included in such a generalization (5.3) a possible dependence of the dissipative scale $\tau_\eta(h)$ on this fluctuating exponent h, that remains to be determined.

The dissipative time scale entering in this formulation (5.3) has a natural dependence on the exponent h. Following the arguments developed for the Eulerian framework by Paladin & Vulpiani (1987), Nelkin (1990) and adapted to the Lagrangian one in Borgas (1993) (and reviewed in Chevillard *et al.* (2012) with corresponding notations), we assume that

$$\tau_\eta(h) = T\left(\frac{\tau_\eta}{T}\right)^{\frac{2}{2h+1}}, \tag{5.4}$$

where, to simplify notations, we call $\tau_\eta \equiv \tau_\eta(1/2)$ the value of the fluctuating dissipative time scale $\tau_\eta(h)$ (5.4) at the very particular value $h = 1/2$. Finally, the fluctuating exponent h is characterized by its probability density function at a given scale τ, namely

$$P_h^{(\tau)}(h) = \frac{1}{\mathcal{Z}(\tau)} \frac{\left(1-\mathrm{e}^{-\frac{\tau}{T}}\right)^{1-\mathcal{D}^L(h)}}{\left[1+\left(\dfrac{\tau}{\tau_\eta(h)}\right)^{-\delta}\right]^{(D^L(h)-1)/\delta}} \tag{5.5}$$

normalized in an appropriate manner using

$$\mathcal{Z}(\tau) = \int_{h_{min}}^{h_{max}} \frac{\left(1-\mathrm{e}^{-\frac{\tau}{T}}\right)^{1-\mathcal{D}^L(h)}}{\left[1+\left(\dfrac{\tau}{\tau_\eta(h)}\right)^{-\delta}\right]^{(\mathcal{D}^L(h)-1)/\delta}} \mathrm{d}h. \tag{5.6}$$

In addition to the two obvious free parameters T and τ_η of this model of the second-order structure function (5.3) that will be calibrated in units of T_L and τ_K in a similar fashion as is presented in § 4.4.2, the multifractal formalism (Frisch 1995) requires the introduction of a parameter function $\mathcal{D}^L(h)$. It acquires the status of a singularity spectrum asymptotically at infinite Reynolds number (i.e. when τ_η goes to 0) and then, at vanishing scales, $\tau \to 0$. It eventually governs the level of fluctuations of the exponent h around its average value, that we expect to be $\langle h \rangle = 1/2$. Several forms have been proposed in the literature (see Frisch 1995). We make a simple quadratic choice for $\mathcal{D}^L(h)$, which is known as a log-normal approximation, parametrized by the intermittency coefficient γ^2 (3.25), that reads

$$\mathcal{D}^L(h) = 1 - \frac{(h - 1/2 - \gamma^2)^2}{2\gamma^2}, \tag{5.7}$$

such that we enforce a linear behaviour of $\mathcal{S}_2(\tau)$ with τ in the inertial range (in the appropriate infinite Reynolds number limit). To make a connection with the notations chosen in Chevillard *et al.* (2003), Chevillard *et al.* (2012), this corresponds to $c_1^L = 1/2 + c_2^L$ for $c_2^L = \gamma^2$.

Correspondingly, the correlation function of acceleration $\mathcal{C}_a(\tau)$ can be defined as (half) the derivatives of the second-order structure function (5.8). Using the notation

$$\mathcal{S}_2(\tau) = \frac{1}{\mathcal{Z}(\tau)} \int_{h_{min}}^{h_{max}} \mathcal{Q}(h,\tau)\,\mathrm{d}h, \quad \text{where } \mathcal{Q}(\tau,h) = \frac{\left(1 - \mathrm{e}^{-\frac{\tau}{T}}\right)^{2h+1-\mathcal{D}^L(h)}}{\left[1 + \left(\dfrac{\tau}{\tau_\eta(h)}\right)^{-\delta}\right]^{(2(1-h)+\mathcal{D}^L(h)-1)/\delta}}, \tag{5.8}$$

we get

$$\begin{aligned}\mathcal{C}_a(\tau) = {} & \left(\frac{\mathcal{Z}'(\tau)^2}{\mathcal{Z}(\tau)^3} - \frac{1}{2}\frac{\mathcal{Z}''(\tau)}{\mathcal{Z}(\tau)^2}\right) \int_{h_{min}}^{h_{max}} \mathcal{Q}(h,\tau)\,\mathrm{d}h - \frac{\mathcal{Z}'(\tau)}{\mathcal{Z}(\tau)^2} \int_{h_{min}}^{h_{max}} \frac{\partial \mathcal{Q}(h,\tau)}{\partial \tau}\,\mathrm{d}h \\ & + \frac{1}{2\mathcal{Z}(\tau)} \int_{h_{min}}^{h_{max}} \frac{\partial^2 \mathcal{Q}(h,\tau)}{\partial \tau^2}\,\mathrm{d}h.\end{aligned} \tag{5.9}$$

The form given in (5.9) can be then considered as a model for the correlation function of acceleration, at a given Reynolds number (which can be estimated as the value of $(T/\tau_\eta)^2$), and that includes intermittent corrections (using a non-vanishing value for γ^2). Remaining integrals entering in (5.9) are evaluated numerically using standard numerical integration algorithms.

5.2.2. *Higher-order structure functions and their scaling behaviour*

Let us give the corresponding prediction for the structure function $\mathcal{S}_{2m}(\tau)$ of order $2m$, that will eventually enter into the expression for the velocity increment flatness. Note that statistics of the increment are expected and observed to be symmetrical, making odd-order moments vanish. It reads

$$\mathcal{S}_{2m}(\tau) = \langle (\delta_\tau v)^{2m} \rangle = (\sqrt{2}\sigma)^{2m} \frac{(2m)!}{m! 2^m} \int_{h_{min}}^{h_{max}} \frac{\left(1 - \mathrm{e}^{-\frac{\tau}{T}}\right)^{2mh}}{\left[1 + \left(\dfrac{\tau}{\tau_\eta(h)}\right)^{-\delta}\right]^{\frac{2m(1-h)}{\delta}}} \mathcal{P}_h^{(\tau)}(h)\,\mathrm{d}h, \tag{5.10}$$

where the additional combinatorial factor originates from the moment of order $2m$ of a zero-average unit-variance Gaussian random variable that enters in the more complete probabilistic description detailed in Chevillard *et al.* (2012).

In the dissipative range, such that $\tau \ll \tau_\eta$, $\mathcal{S}_{2m}(\tau)$ (5.10) behaves in a consistent manner with its Taylor development, that is $\mathcal{S}_{2m}(\tau) = \langle a^{2m}\rangle \tau^{2m} + o(\tau^{2m})$. In the inertial range, i.e. for $\tau_\eta \ll \tau \ll T$, we recover the standard prediction of the multifractal formalism, that relates the power-law behaviour of the structure functions to the functional shape of the parameter function $\mathcal{D}^L(h)$ through a Legendre transform (Frisch 1995). We have, in the proper ordering of limits,

$$\lim_{\tau_\eta\to 0} \mathcal{S}_{2m}(\tau) \underset{\tau\to 0}{\sim} c_{\gamma,2m}(\sqrt{2}\sigma)^{2m} \frac{(2m)!}{m!2^m} \left(\frac{\tau}{T}\right)^{min_h[2mh+1-\mathcal{D}^L(h)]}, \tag{5.11}$$

where the remaining multiplicative constant could be computed while pushing forward the underlying steepest-descent calculation techniques that we develop in § 5.2.3. Assuming then a quadratic form for the parameter function $\mathcal{D}^L(h)$ (5.7), once again this could be done for other choices (Frisch 1995), we obtain the following intermittent behaviour

$$\lim_{\tau_\eta\to 0} \mathcal{S}_{2m}(\tau) \underset{\tau\to 0}{\sim} c_{\gamma,2m}(\sqrt{2}\sigma)^{2m} \frac{(2m)!}{m!2^m} \left(\frac{\tau}{T}\right)^{(1+2\gamma^2)m-2\gamma^2m^2}, \tag{5.12}$$

which power-law exponent $\zeta_{2m} \equiv (1+2\gamma^2)m - 2\gamma^2m^2$ corresponds exactly to the one obtained for the infinitely differentiable multifractal random walk of § 3.2 (where the scaling behaviour of its structure functions at infinite Reynolds number can be found in Proposition A.6).

5.2.3. *Derivation of the Reynolds number dependence of the acceleration variance*

We now give the Reynolds number dependence, or equivalently the dependence on the free parameters τ_η and T, of the acceleration variance, and the scaling behaviour of $\mathcal{S}_{2m}(\tau)$ with τ at infinite Reynolds number (i.e. for $\tau_\eta \to 0$). As detailed in Chevillard *et al.* (2012), or simply deduced from (5.10) using $\mathcal{S}_2(\tau) = \langle a^2\rangle\tau^2 + o(\tau^2)$, we have

$$\langle a^2\rangle = \frac{2\sigma^2}{T^2}\frac{1}{\mathcal{Z}(0)}\int_{h_{min}}^{h_{max}} \left(\frac{\tau_\eta}{T}\right)^{2\frac{2(h-1)+1-\mathcal{D}^L(h)}{2h+1}} \mathrm{d}h, \tag{5.13}$$

with

$$\mathcal{Z}(0) = \int_{h_{min}}^{h_{max}} \left(\frac{\tau_\eta}{T}\right)^{2\frac{1-\mathcal{D}^L(h)}{2h+1}} \mathrm{d}h. \tag{5.14}$$

Follow then a steepest-descent procedure. Compute first the minimum and the minimizer of the exponents entering in (5.13) and (5.14), using for $\mathcal{D}^L$ the expression provided in (5.7). Notice that $min_h((1-\mathcal{D}^L(h))/(2h+1)) = 0$ and assume $\gamma^2 < 2-\sqrt{3}$ to guarantee the positivity of these real-valued minimizers, a condition which is fulfilled by the empirical value of the intermittency coefficient (3.25). To get an estimation of the remaining multiplicative constant following this steepest-descent calculation, perform a Taylor series of the exponents entering in (5.13) and (5.14) around their respective minimizer up to second order, and finally approximate the remaining Gaussian integrals extending the integration range over $h \in \mathbb{R}$. We eventually obtain the following exact equivalent as the Reynolds number goes to infinity:

$$\langle a^2 \rangle \underset{\tau_\eta \to 0}{\sim} \frac{2\sigma^2}{T^2} \frac{[1-4\gamma^2+\gamma^4]^{\frac{1}{4}}}{\sqrt{1+\gamma^2}} \left(\frac{\tau_\eta}{T}\right)^{\frac{\gamma^2-1+\sqrt{1-4\gamma^2+\gamma^4}}{\gamma^2}}. \tag{5.15}$$

We can see that the multifractal prediction of acceleration variance (5.15) does exhibit an intermittent correction, as was already derived in a very similar way by Borgas (1993) and Sawford *et al.* (2003). For a more detailed comparison with DNS data, we invite the reader to § 5.3. At this stage, we notice that, whereas structure functions at infinite Reynolds number obtained from the multifractal formalism (5.12) and from the infinitely differentiable MRW (Proposition A.6) behave in a very similar way, predicted acceleration variances differ by intermittent corrections (compare (5.15) and (A 34)).

5.3. *Calibration of the free parameters and comparisons with DNS data*

We adopt the same calibration of the free parameters τ_η and T as depicted in § 4.4.2. We numerically solve the nonlinear problem consisting of obtaining τ_η and T from the empirical value of T_L and the appropriate zero crossing of acceleration time scale given in units of τ_K. It is thus very similar to solving the system of (4.5) and (4.6), but notice there that, moreover, the integral time scale T_L predicted from the model has to be computed numerically using a standard integration scheme of the expression provided in (5.3). To give a hint to the numerical algorithm that looks for zeros of functions, as is required while solving this nonlinear problem, we can make a simple prediction for the zero crossing of acceleration time scale τ_0. Using Batchelor's parametrization of the second-order structure function (5.1), and the corresponding prediction of the acceleration correlation function (5.2), we expect that a good approximation of τ_0 would be given by

$$\tau_0 \underset{\tau_\eta \to 0}{\approx} \tau_\eta \left(\frac{\delta-1}{2}\right)^{-\frac{1}{\delta}}, \tag{5.16}$$

showing that, indeed, the free parameter τ_η is expected to be proportional to the Kolmogorov dissipative time scale τ_K.

Using the physical parameters of the DNS data provided in table 1, assuming furthermore $\gamma^2 = 0.085$ (3.25) and $\delta = 4$, we look for the solution of this aforementioned nonlinear system of equations (similar to (4.5) and (4.6)). We finally retrieve $(\tau_\eta/\tau_K, T/T_L) = (2.7596, 0.9927)$ for $\mathcal{R}_\lambda = 185$, and $(2.6106, 0.9983)$ for $\mathcal{R}_\lambda = 418$.

Having in hand the calibrated values for the parameters τ_η and T, we now compare with DNS data. Similar to figure 4(*a–c*) we represent in figure 5(*a–c*) the predictions of the velocity correlation function $\mathcal{C}_v(\tau)$, the second-order structure function $\mathcal{S}_2(\tau)$ and the acceleration correlation function $\mathcal{C}_a(\tau)$, all based on the multifractal parametrization of the second-order structure function (5.3), and its second derivative (5.9). As far as velocity is concerned, we observe a perfect agreement between predictions and DNS data, for both correlation (figure 5*a*) and second-order structure function (figure 5*b*).

Concerning the acceleration correlation function $\mathcal{C}_a(\tau)$ (figure 5*c*), we observe that predictions overestimate slightly the observed negative values after the zero crossing. Interestingly, we observed an opposite behaviour with the former depicted infinitely differentiable process (figure 4*c*). Below the zero-crossing time scale, predictions overestimate the decrease of correlation, although the dependence on the Reynolds number

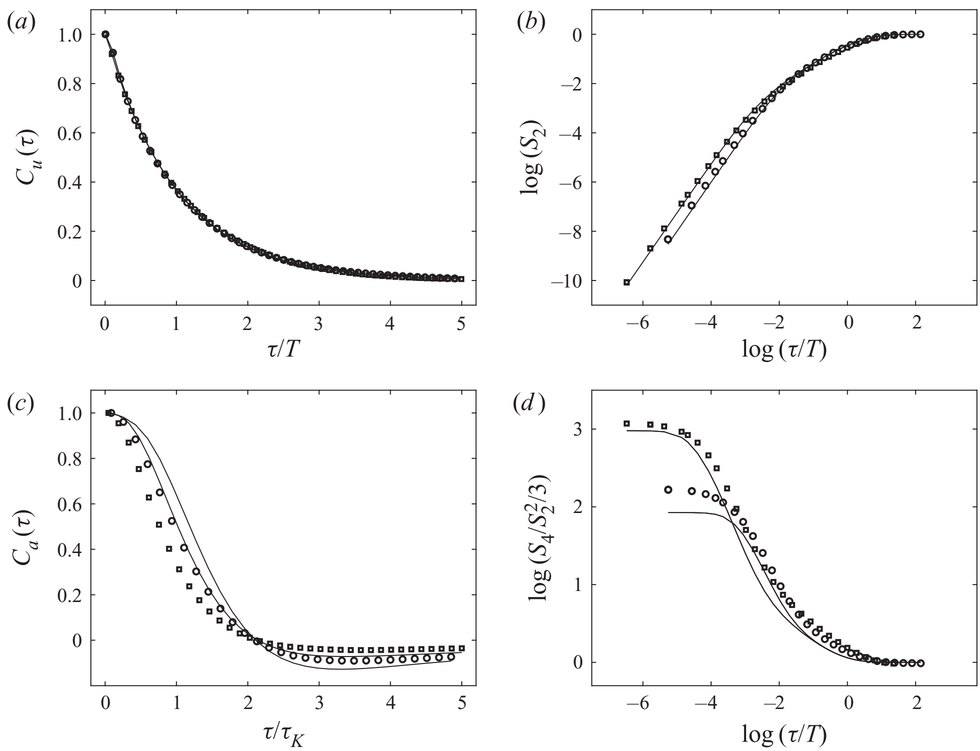

FIGURE 5. Comparison of DNS data with model predictions, similar to figure 4, but for multifractal predictions. (*a*) Estimation of the velocity correlation function from DNS data (○ and □ as in figure 4). We superimpose theoretical predictions based on the multifractal parametrization of the second-order structure function (5.3), for the set of values of the parameters τ_η and T given by our calibration procedure presented in § 5.3, and for a prescribed value for γ (3.25) and $\delta = 4$. Time lags are normalized by the calibrated time scale T. (*b*) Same plot as in (*a*) but for the second-order structure function. (*c*) Similar plot as in (*a*,*b*) but for the acceleration correlation function, normalized by its value at the origin. Superimposed theoretical predictions are based on the exact expression given in (5.9). (*d*) Similar plot as in (*a*,*b*) but for the corresponding flatnesses of velocity increments. Theoretical predictions are obtained from the expression given in (5.10).

goes in the good direction. Compared with the performance of the stochastic process depicted in § 3.2, and displayed in figure 4(*c*), we can see that predictions based on the multifractal formalism do not perform as well. As we will see, the strength of the multifractal formalism lies in the possibility of understanding and modelling the rapid increase of the flatness in the intermediate dissipative range. We are thus led to the conclusion that this rapid increase, coming from the differential action of viscosity, does not explain the discrepancies that we can observe between DNS and models.

We now focus on the intermittency corrections, as is well quantified by the flatness of velocity increments. We compare in figure 5(*d*) the flatness of increments, based on DNS and on the current multifractal model using the expression given in (5.10). We can see that multifractal predictions reproduce accurately the overall shape of the flatness, including the rapid increase in the intermediate dissipative range, for both Reynolds numbers. Recall that this very dissipative behaviour is not reproduced by the stochastic approach of § 3.2, and displayed in figure 4(d), We can notice furthermore a slight shift between the numerical and theoretical curves: this indicates that the large time scale associated with intermittent corrections is slightly larger than the one associated with the velocity correlation time scale. This could be included in the expressions of structure functions ((5.3) and (5.10)) at the price of introducing another *ad hoc* free parameter of order unity, without further justifications (data not shown). Nonetheless, we can see that, overall, the present multifractal model reproduces in good agreement DNS data, both in the inertial and dissipative ranges.

Going back to the predicted variance of the acceleration (5.15) and its comparison with data, we will articulate this discussion around the compilation of DNS data at various Reynolds numbers performed by Ishihara *et al.* (2007), and the comparison with an empirical form proposed by Hill (2002). To make the discussion short and simple, we use the prescribed value for γ (3.25), and write the predicted variance (5.15) as $\langle a^2\rangle \propto (\sigma/T)^2(\tau_\eta/T)^{-1-0.155}$, which is the standard non-intermittent phenomenological prediction, enhanced by an intermittent correction of order $(\tau_\eta/T)^{-0.155}$. The calibration procedure used here confirms that τ_η has, to a good approximation, the same Reynolds number dependence as τ_K. Furthermore, T is very close to T_L, such that $T \propto L/\sigma$, where L is the large length scale of the flow, and recall that σ is the velocity standard deviation. Using $\langle\varepsilon\rangle \propto \sigma^3/L$, we can rewrite the empirical form for $\langle a^2\rangle$ proposed by Ishihara *et al.* (2007) (see their equation 5.10 and the respective discussion) in units of $(\sigma/T)^2$. This empirical form of Ishihara *et al.* (2007) consists in the sum of two power laws, a dominant one at large Reynolds numbers of order $(\sigma/T)^2(\tau_\eta/T)^{-1.25}$, and a subdominant one of order $(\sigma/T)^2(\tau_\eta/T)^{-1.11}$. We can see that the present theoretical prediction, i.e. $(\sigma/T)^2(\tau_\eta/T)^{-1.155}$, using (5.15) with the prescribed value for γ (3.25) lies in between these two power laws. As we noticed in § 5.2.3, such a prediction of the multifractal formalism has already been derived by Borgas (1993) and Sawford *et al.* (2003), and compared with a compilation of DNS data in Sawford *et al.* (2003) and Yeung *et al.* (2006): derived in a very similar way as we do, although based on a different choice for the parameter function $\mathcal{D}^L(h)$ (5.7), the acceleration variance was predicted to behave as $(\sigma/T)^2(\tau_\eta/T)^{-1.135}$, which is very close to the present prediction, and was shown to reproduce accurately the trends observed in DNS. We are led to the conclusion that, given the available range of Reynolds numbers accessible in DNS, corrections to standard phenomenological arguments for the acceleration variance as they are observed in DNS data are consistent with implied corrections by the intermittency phenomenon.

5.4. *Further considerations regarding the prediction of the multifractal formalism*

Here, we develop the model of the differential action of viscosity and the implied dependence of the dissipative length and time scales on the local exponent h, as is proposed in particular in Paladin & Vulpiani (1987), Nelkin (1990) and Borgas (1993). Rephrased in terms of time scales, similar arguments could be developed for length scales, we can estimate the extension of the range on which the dissipative time scale $\tau_\eta(h)$ varies. Actually, it will turn out to be more appropriate to estimate this range in a logarithmic fashion. This is due to the fact that the probability density function of $\log(\tau_\eta(h)/T)$ is eventually very close to a Gaussian function as $\tau_\eta/T \to 0$, and is thus well characterized by its average and standard deviation. Using (5.4), we get

$$\log\left(\frac{\tau_\eta(h)}{T}\right) = \frac{2}{2h+1}\log\left(\frac{\tau_\eta}{T}\right), \tag{5.17}$$

such that the respective moments of order $q \in \mathbb{N}$ are given by,

$$\left\langle \left(\log \left(\frac{\tau_\eta(h)}{T} \right) \right)^q \right\rangle = \frac{1}{\mathcal{Z}(0)} \int_{h_{min}}^{h_{max}} \left(\frac{2}{2h+1} \right)^q \left(\frac{\tau_\eta}{T} \right)^{\frac{2[1-\mathcal{D}^L(h)]}{2h+1}} \mathrm{d}h \, \log^q \left(\frac{\tau_\eta}{T} \right), \tag{5.18}$$

where the normalization constant $\mathcal{Z}(0)$ is defined as the limit when $\tau \to 0$ of the expression given in (5.6). To simplify expressions, and work with explicit functions instead of integrals, assume for this discussion $h_{min} = -1/2$ and $h_{max} = +\infty$. Make the change of variable $x = (2h+1)/2$ to obtain

$$\left\langle \left(\log \left(\frac{\tau_\eta(h)}{T} \right) \right)^q \right\rangle = \frac{1}{\mathcal{Z}(0)} \int_0^\infty \frac{1}{x^q} \left(\frac{\tau_\eta}{T} \right)^{\frac{1-\mathcal{D}^L(x-1/2)}{x}} \mathrm{d}x \, \log^q \left(\frac{\tau_\eta}{T} \right). \tag{5.19}$$

Assuming then for $\mathcal{D}^L$ a quadratic approximation (5.7) with given parameter γ^2, using a symbolic calculation software, we obtain as $\tau_\eta/T \to 0$

$$\left\langle \log \left(\frac{\tau_\eta(h)}{T} \right) \right\rangle = \frac{1}{1+\gamma^2} \log \left(\frac{\tau_\eta}{T} \right) + O(1), \tag{5.20}$$

and

$$\left\langle \left(\log \left(\frac{\tau_\eta(h)}{T} \right) \right)^2 \right\rangle - \left\langle \log \left(\frac{\tau_\eta(h)}{T} \right) \right\rangle^2 = \frac{\gamma^2}{(1+\gamma^2)^3} \log \left(\frac{T}{\tau_\eta} \right) + O(1). \tag{5.21}$$

Keeping in mind that $\gamma^2 = 0.085$ (3.25) remains small compared with unity, these former considerations show that, in a logarithmic representation, the dissipative time scale fluctuates over an extended range, centred on a time scale close to $\log \tau_\eta$ (5.20), and of width proportional to $\sqrt{\log(T/\tau_\eta)}$ (5.21), or equivalently proportional to $\sqrt{\log \mathcal{R}_e}$. The extension of such an intermediate dissipative range and its respective Reynolds number dependence has been already predicted by similar, although different, arguments in Chevillard *et al.* (2005). It is here re-derived based on the multifractal modelling using (5.4). Although such a predicted extension of the intermediate dissipative range (a width that behaves as $\sqrt{\log \mathcal{R}_e}$ in this logarithmic representation) can be considered as large, it differs in nature from, and is narrower than, other predictions. For example, Yakhot & Sreenivasan (2005) attributes a dynamical significance to length scales that behave as $\mathcal{R}_{\mathrm{e}}^{-1}$. Such small length scales, once reformulated in a Lagrangian context, have no significance as far as variance of the logarithm of $\tau_\eta(h)$ is concerned, or equivalently at this level of description, as given by the flatness of the velocity increments. Similarly, in Dubrulle (2019), much emphasis is given to the scale obtained while taking $h \to -1/2$ in (5.4) corresponding to a vanishing time scale (or correspondingly in a Eulerian framework, taking $h \to -1$ in the multifractal parametrization of the Kolmogorov dissipative length scale). Once again, the present derivation of the intermediate dissipative range gives no significance to such a small time scale, i.e. its probability of appearance is vanishingly small as the Reynolds number becomes large. Finally, it is claimed in Buaria *et al.* (2019), based on the behaviour of the tails of the probability density functions of the velocity gradients, that much smaller length scales are involved in the dynamics. Once again, the implication of the existence of these very fine length or time scales cannot be quantified using only the flatness of the velocity increments. Actually, extreme events of gradients (or acceleration), as observed in the tails of their probability density, can be modelled using the probabilistic approach of Castaing, Gagne & Hopfinger (1990), as reviewed and related to the language of the multifractal formalism by Chevillard *et al.* (2012).

Let us conclude this digression by justifying our estimation of the width of the intermediate dissipative range based on logarithmic scales (and, incidentally, the moments of the logarithm of the dissipative time scales as given in (5.20) and (5.21)). Further calculations, similar to the ones performed in (5.20) and (5.21) based on a quadratic approximation for $\mathcal{D}^L(h)$ (5.7), show that the respective flatness of $\log(\tau_\eta(h)/T)$ (once centred in an appropriate way) behaves as $3 + O(\log^{-1}(\tau_\eta/T))$, showing that the logarithm of the fluctuating dissipative time scale behaves in an asymptotic way as a Gaussian random variable, thus properly characterized by its mean and variance.

6. Conclusions and perspectives

Let us summarize our original findings in the context of the stochastic modelling of the Lagrangian velocity and acceleration.

First, we have proposed, for the first time as far we know, a stochastic dynamics which is causal, infinitely differentiable at a given Reynolds number, or equivalently to a good approximation, for a given finite ratio of a dissipative time scale τ_η over a large one T. This process, that we called u, is defined as the limit $n \to \infty$ of the n-layered embedded process u_n ((3.8)–(3.12)). Its second-order statistical properties are derived analytically and results are gathered in Proposition A.5. We furthermore included in a causal and exact way some intermittent properties, given an intermittent coefficient γ (3.25). As intermittency disappears, i.e. if we take $\gamma = 0$, we recover a Gaussian process that we noted by v, of which the causal dynamics is discussed in § 2.3, and of which the second-order statistical properties are listed in Proposition A.2. At infinite Reynolds number, i.e. when $\tau_\eta \to 0$, both processes converge towards a statistically stationary and finite-variance causal process, which is a (Gaussian) Ornstein–Uhlenbeck process concerning v and a multifractal random walk concerning u. As far as the multifractal version u is concerned, we have computed in an exact fashion the intermittent behaviour of its structure functions, and results are gathered in Proposition A.6. Using an efficient algorithm designed in § 3.3.1, we have shown that such processes are easily to simulate, and we have been able to compare with great success our theoretical predictions with numerical simulations of the underlying dynamics.

We have then analysed Lagrangian trajectories extracted from a set of DNS of the Navier–Stokes equations (see table 1 where important physical parameters of the simulations are gathered) and compared their statistical properties with those of u in figure 4. Following a calibration procedure (§ 4.4.2) that relates in a transparent and reproducible way the free parameters of the model τ_η and T to the empirical values of the Kolmogorov time scale τ_K and of the integral one T_L, we are then able to reproduce with great accuracy the statistical properties of the DNS trajectories. We nonetheless observed some discrepancies below the zero-crossing time scale of the acceleration correlation function (figure 4*c*), and the flatness of velocity increments at similar dissipative time scales (figure 4*d*).

To push forward our understanding of the observed rapid increase of the flatness in the intermediate dissipative range, and on the way explore some new types of prediction for the acceleration correlation function, we have recalled and developed a phenomenological procedure mostly based on the multifractal formalism (see § 5). This alternative approach differs from building up a stochastic process, as was done for u. Instead, it proposed the modelling of the some chosen statistical properties such as structure functions. Nonetheless, it allows for the derivation of new predictions for the acceleration correlation function and flatness of the velocity increments, that reproduce in a very accurate way DNS data (see the proposed discussions on the results displayed in figure 5*c*,*d*). In particular, the theoretically predicted flatness reproduces its rapid increase in the intermediate dissipative range, a phenomenon that is related to the differential action of viscosity depending on the local singular strength of velocity, as modelled by the parametrization of Paladin & Vulpiani (1987), Nelkin (1990) and Borgas (1993).

It would be useful, from a modelling perspective, to analyse a specifically designed DNS, and its Lagrangian trajectories, where special care has been taken to resolve in an appropriate way the range of dissipative scales. Also, at the price of being limited in terms of Reynolds numbers, it would be much appreciated to work with numerous trajectories, each of them lasting far longer that the Lagrangian integral time scale T_L. Only then would we be able to discriminate between schematic modelling aspects and a lack of numerical resolution. Also, both current theoretical approaches shed new light on the interpretation of experimental data in this range of time scales where viscosity dominates, and open the route to an original characterization of the influence of possible large scale anisotropic situations. Finally, it would be welcome, from the theoretical side, to include this differential action of viscosity as modelled by Paladin & Vulpiani (1987), Nelkin (1990) and Borgas (1993) into the stochastic approach that ends up with u and developed in § 3.2. To date, we do not know how to model in a stochastic manner (and to provide the respective causal dynamics) this tricky action of viscosity; we can nonetheless conclude that a simple linear filtering at small scales fails at reproducing such a behaviour. A natural idea would be to weight the filtering at the scale of order τ_η by a function of the multifractal random field. This remains to be explored and we leave these aspects for future investigations.

Acknowledgements

The authors thank the PSMN (Pôle Scientifique de Modélisation Numérique) computing centre of ENS de Lyon for numerical resources. We thank J. Bec, L. Biferale and F. Toschi for providing and making available DNS data. Similarly, we thank those involved in curating and maintaining the JHTDB. B.V. and R.B.C. are supported by U.S. National Science Foundation grant (GEO-1756259). R.B.C. is also thankful for the support provided through the Fulbright Scholar Program. J.F. acknowledges funding from the Humboldt Foundation within a Feodor-Lynen fellowship. B.V., J.F., R.V., M.B., L.C. benefit from the financial support of the Project IDEXLYON of the University of Lyon in the framework of the French programme 'Programme Investissements d'Avenir' (ANR-16-IDEX-0005). L.C. is supported by ANR grants LIOUVILLE ANR-15-CE40-0013 and by the Simons Foundation Award ID: 651475.

Declaration of interests

The authors report no conflict of interest.

Appendix A. Propositions concerning infinitely differentiable causal stochastic processes

PROPOSITION A.1. *Assume* $n \geq 2$. *Then the correlation functions of velocity and acceleration are given by*

$$\mathcal{C}_{v_n}(\tau) = q_{(n)} \left(G_T \star G_{\tau_\eta}^{\star(n-1)} \right)(\tau), \tag{A 1}$$

and

$$\mathcal{C}_{a_n}(\tau) = -\frac{\mathrm{d}^2\mathcal{C}_{v_n}(\tau)}{\mathrm{d}\tau^2}, \tag{A 2}$$

where we have introduced the correlation product $\star$, which is defined as, for any two functions g_1 and g_2,

$$(g_1 \star g_2)(\tau) = \int_{\mathbb{R}} g_1(t)g_2(t+\tau)\,\mathrm{d}t,$$

with the corresponding shorthand notation,

$$g^{\star n} = \underbrace{g \star g \star \cdots \star g}_{n},$$

and the response function of the OU process at a given time scale τ (here $\tau = T$ or $\tau = \tau_\eta$)

$$t \in \mathbb{R} \mapsto G_\tau(t) = \frac{\tau}{2}\mathrm{e}^{-|t|/\tau}. \tag{A 3}$$

For the sake of completeness, we also provide the spectral view of the correlation functions of velocity and acceleration, ((A 1) and (A 2)), which is especially useful when seeking their explicit expression for a given layer n, once injected into a symbolic calculation software. We have

$$\mathcal{C}_{v_n}(\tau) = q_{(n)} \int_{\mathbb{R}} \mathrm{e}^{2\mathrm{i}\pi\omega\tau} \frac{T^2}{1+4\pi^2T^2\omega^2}\left[\frac{\tau_\eta^2}{1+4\pi^2\tau_\eta^2\omega^2}\right]^{n-1} \mathrm{d}\omega, \tag{A 4}$$

and

$$\mathcal{C}_{a_n}(\tau) = q_{(n)} \int_{\mathbb{R}} 4\pi^2\omega^2\mathrm{e}^{2\mathrm{i}\pi\omega\tau} \frac{T^2}{1+4\pi^2T^2\omega^2}\left[\frac{\tau_\eta^2}{1+4\pi^2\tau_\eta^2\omega^2}\right]^{n-1} \mathrm{d}\omega. \tag{A 5}$$

To finish with this proposition, we state the implied expression for the constant $q_{(n)}$ to ensure the physical constraint on velocity variance (2.19) by Parseval's identity,

$$\frac{\sigma^2}{q_{(n)}} = \int_{\mathbb{R}} \frac{T^2}{1+4\pi^2T^2\omega^2}\left[\frac{\tau_\eta^2}{1+4\pi^2\tau_\eta^2\omega^2}\right]^{n-1} \mathrm{d}\omega. \tag{A 6}$$

Proof. Rephrased in the language of linear systems theory (see for instance Papoulis 1991), the system of equations (2.14)–(2.18) defines a series of linear filters with a stochastic input. This explains the expression given for the velocity correlation of v_n (A 1).

We compute the correlation function of v_n, as was done in (2.11) in a more straightforward manner, and drawing a connection with the approach adopted to present the model of Sawford (§ 2.2.1). We obtain

$$\mathcal{C}_{v_n}(\tau) = \int_{-\infty}^{0}\int_{-\infty}^{\tau} \mathrm{e}^{-(\tau-t_1-t_2)/T}\mathcal{C}_{f_{n-1}}(t_1-t_2)\,\mathrm{d}t_1\,\mathrm{d}t_2,$$

which can be formally rewritten as

$$\begin{aligned}\mathcal{C}_{v_n}(\tau) &= \int_{\mathbb{R}^2} g_T(\tau+t_2)g_T(t_1)\mathcal{C}_{f_{n-1}}(t_1-t_2)\,\mathrm{d}t_1\,\mathrm{d}t_2\\ &= \int_{\mathbb{R}^2} g_T(\tau+t_1+t_2)g_T(t_1)\mathcal{C}_{f_{n-1}}(t_2)\,\mathrm{d}t_1\,\mathrm{d}t_2\end{aligned}$$

$$= \int_{\mathbb{R}} (g_T \star g_T)(\tau + t_2)\mathcal{C}_{f_{n-1}}(t_2)\, \mathrm{d}t_2$$
$$= \left(g_T \star g_T \star \mathcal{C}_{f_{n-1}}\right)(\tau),$$

where $g_T(t) = \mathrm{e}^{-t/T} 1_{t\geq 0}$. Noticing that $G_T(t) = (g_T \star g_T)(t)$, we arrive at the proposition made in (A 1) after iterating the procedure for the $n-1$ remaining layers. The equivalent form of the velocity correlation in the spectral space (A 4) is a consequence of the convolution theorem, and that the Fourier transform of G_T is a Lorentzian function. □

PROPOSITION A.2. *Take $n \geq 2$. Using the results of Proposition A.1, we have*

$$\mathcal{C}_{v_n}(\tau) = \frac{2\sigma^2 \mathrm{e}^{-\tau_\eta^2/T^2}}{T \mathrm{erfc}\left(\tau_\eta/T\right)} \int_{\mathbb{R}} \mathrm{e}^{2i\pi\omega\tau} \frac{T^2}{1+4\pi^2 T^2\omega^2} \left[\frac{1}{1+\dfrac{4\pi^2\tau_\eta^2\omega^2}{n-1}}\right]^{n-1} \mathrm{d}\omega, \tag{A 7}$$

such that

$$\mathcal{C}_{v}(\tau) \equiv \lim_{n\to\infty} \mathcal{C}_{v_n}(\tau) = \frac{2\sigma^2 \mathrm{e}^{-\tau_\eta^2/T^2}}{T \mathrm{erfc}\left(\tau_\eta/T\right)} \int_{\mathbb{R}} \mathrm{e}^{2i\pi\omega\tau} \frac{T^2}{1+4\pi^2 T^2\omega^2} \exp(-4\pi^2\tau_\eta^2\omega^2)\, \mathrm{d}\omega. \tag{A 8}$$

We get

$$\mathcal{C}_{v}(\tau) = \sigma^2 \frac{\mathrm{e}^{-|\tau|/T}}{2\mathrm{erfc}(\tau_\eta/T)} \left[1 + erf\left(\frac{|\tau|}{2\tau_\eta} - \frac{\tau_\eta}{T}\right) + \mathrm{e}^{2|\tau|/T}\mathrm{erfc}\left(\frac{|\tau|}{2\tau_\eta} + \frac{\tau_\eta}{T}\right)\right], \tag{A 9}$$

with the particular value $\mathcal{C}_v(0) = \langle v^2\rangle = \sigma^2$. Concerning the acceleration correlation function, take (minus) the second derivative of $\mathcal{C}_v$ (A 9) and we obtain

$$\mathcal{C}_{a}(\tau) = \frac{\sigma^2}{2T^2\mathrm{erfc}(\tau_\eta/T)} \left[\frac{2T}{\tau_\eta\sqrt{\pi}} \exp\left(-\left(\frac{\tau^2}{4\tau_\eta^2} + \frac{\tau_\eta^2}{T^2}\right)\right) - \mathrm{e}^{-|\tau|/T}\left(1 + \mathrm{erf}\left(\frac{|\tau|}{2\tau_\eta} - \frac{\tau_\eta}{T}\right)\right)\right.$$
$$\left. -\mathrm{e}^{|\tau|/T}\mathrm{erfc}\left(\frac{|\tau|}{2\tau_\eta} + \frac{\tau_\eta}{T}\right)\right]. \tag{A 10}$$

Proof. By Lebesgue's dominated convergence, we can safely commute $\lim_{n\to\infty}$ and the indefinite integral that enter in the expression given in (A 7). Recall that $(1 + x/n)^n$ tends to e^x as $n \to \infty$, and we get to (A 8). Express then (A 8) in the physical space as a convolution, and perform the remaining integral to arrive at (A 9). The expression in (A 10), the acceleration correlation function, also follows. □

PROPOSITION A.3 (On the statistical properties of the fields $X_{1,\epsilon}$ and its asymptotical log-correlated version $X_1 \equiv \lim_{\epsilon\to 0} X_{1,\epsilon}$). *Recall first the definition of the OU-kernel $g_\tau(t) = \mathrm{e}^{-t/\tau} 1_{t\geq 0}$, where $1_{t\geq 0}$ stands for the indicator function of positive reals, and the associated response function $G_\tau(t) = (g_\tau \star g_\tau)(t) = (\tau/2)\mathrm{e}^{-|t|/\tau}$ (A 3). We will also need its derivative, which reads as $G'_\tau(t) = -(t/(2|t|))\mathrm{e}^{-|t|/\tau}$.*

The unique solution $X_{1,\epsilon}$ of the dynamics given in (3.2) is a zero-average Gaussian process that reaches a statistically stationary regime at large time t, independently of the *initial condition. In this statistically steady state, $X_{1,\epsilon}$ is thus fully characterized by its correlation function that reads*

$$\mathcal{C}_{X_{1,\epsilon}}(\tau) = -\int_0^\infty \left[G_T'(\tau+h) - G_T'(\tau-h)\right] \frac{\mathrm{d}h}{h+\epsilon+\sqrt{\epsilon(h+\epsilon)}} \tag{A 11}$$

$$= -\mathrm{e}^{-|\tau|/T}\int_0^{|\tau|} \frac{\sinh(h/T)\,\mathrm{d}h}{h+\epsilon+\sqrt{\epsilon(h+\epsilon)}} + \cosh(|\tau|/T)\int_{|\tau|}^\infty \frac{\mathrm{e}^{-h/T}\,\mathrm{d}h}{h+\epsilon+\sqrt{\epsilon(h+\epsilon)}}. \tag{A 12}$$

In particular, we have

$$\mathcal{C}_{X_{1,\epsilon}}(0) = \langle X_{1,\epsilon}^2\rangle = \int_0^\infty \frac{\mathrm{e}^{-h/T}\,\mathrm{d}h}{h+\epsilon+\sqrt{\epsilon(h+\epsilon)}} \tag{A 13}$$

$$\underset{\epsilon\to 0}{=} \log\left(\frac{1}{\epsilon}\right) + O(1). \tag{A 14}$$

In the asymptotic regime $\epsilon \to 0$, whereas the variance of $X_{1,\epsilon}$ diverges, its correlation function at a given time lag $|\tau| > 0$ remains a bounded function of ϵ. This defines an asymptotic zero-average Gaussian process X_1 of infinite variance, but with a bounded covariance for $|\tau| > 0$. We obtain

$$\mathcal{C}_{X_1}(\tau) = \lim_{\epsilon\to 0}\mathcal{C}_{X_{1,\epsilon}}(\tau) = -\int_0^\infty \left[G_T'(\tau+h) - G_T'(\tau-h)\right]\frac{\mathrm{d}h}{h} \tag{A 15}$$

$$= -\mathrm{e}^{-|\tau|/T}\int_0^{|\tau|}\sinh(h/T)\frac{\mathrm{d}h}{h} + \cosh(|\tau|/T)\int_{|\tau|}^\infty \mathrm{e}^{-h/T}\frac{\mathrm{d}h}{h} \tag{A 16}$$

$$= \log^+\left(\frac{T}{|\tau|}\right) + c(|\tau|), \tag{A 17}$$

where $\log^+(x) = \log(\max(x, 1))$ and $c(|\tau|)$ is a bounded function of its argument such that it goes to zero as $|\tau| \to \infty$. Of special interest is the value of c at the origin. We obtain

$$c(0) = \int_0^\infty \mathrm{e}^{-y}\log(y)\,\mathrm{d}y \approx -0.577216, \tag{A 18}$$

and is known as (minus) the Euler–Mascheroni constant.

The corresponding spectral representation of the correlation function of the limiting process X_1 is given by

$$\mathcal{C}_{X_1}(\tau) = \int_{\mathbb{R}} \mathrm{e}^{2i\pi\omega\tau}2\pi^2|\omega|\frac{T^2}{1+4\pi^2T^2\omega^2}\,\mathrm{d}\omega. \tag{A 19}$$

Proof. Arguments developed in Chevillard (2017) can be easily adapted to show the expression of the correlation function of $X_{1,\epsilon}$ at a given finite ϵ ((A 11) and (A 12)) (see Pereira *et al.* (2018) for a full derivation). The expression of its variance (A 13) is a consequence of (A 12). To see the logarithmic divergence with respect to ϵ (A 14), split the integral entering in (A 13) in two over $[0, \epsilon]$ and $[\epsilon, \infty]$ and observe that the first term tends to a bounded constant as $\epsilon \to 0$. Subtract then from the second term the quantity $\int_\epsilon^\infty \mathrm{e}^{-h/T}\,\mathrm{d}h/h$ and observe that the overall quantity remains bounded as $\epsilon \to 0$. This shows the logarithmic divergence since this is the case for this subtracted quantity (performing an integration by parts over the dummy variable h).

Similarly, expressions for the correlation function of the limiting process X_1 ((A 15) and (A 16)) are shown in Chevillard (2017) and Pereira *et al.* (2018). Remark that the first integral on the right-hand side of (A 16) vanishes as $\tau \to 0$, and observe (again by integration by parts) that the second integral diverges logarithmically with τ, showing the small scale diverging behaviour depicted in (A 17). To prove the overall shape of $\mathcal{C}_{X_1}$ as it is given in (A 17), we have to show that the function c is indeed bounded and goes to zero at large arguments. It is easy to see that once the logarithmic diverging behaviour is subtracted from the full expression, only bounded terms remain, which makes c bounded too. At large arguments, re-organize the terms in a proper way to see the convergence towards zero.

To show the spectral representation of the correlation function (A 19), use $G'_T(t) = \int \mathrm{e}^{2\,\mathrm{i}\pi\omega t} 2i\pi\omega T^2/(1+4\pi^2\omega^2T^2)\,\mathrm{d}\omega$ and inject into (A 15). Perform then the remaining integral over the dummy variable h using the known result $\int_0^\infty \sin(u)/u\,\mathrm{d}u = \pi/2$, and we get (A 19). As a final remark, whereas the regularization procedure over ϵ used in (3.2) may appear somehow arbitrary, and has some impact on the functional form of the correlation function $\mathcal{C}_{X_{1,\epsilon}}(\tau)$ ((A 11) and (A 12)), this dependence disappears in the limit $\epsilon \to 0$. In other words, the same correlation function $\mathcal{C}_{X_1}(\tau)$ ((A 15) and (A 16)) would have been obtained using another regularization procedure as long as the divergent behaviours of variance (A 14) and covariance (A 17) are ensured. This canonical behaviour of the limiting process X_1 is consistent with the conclusions of Robert & Vargas (2010) and Rhodes & Vargas (2014). □

PROPOSITION A.4. (On the statistical properties of the field $X_{n,\epsilon}$ and its asymptotical behaviour). *The unique solution $X_{n,\epsilon}$ of the dynamics given in (3.14) is a zero-average Gaussian process, and reaches a statistically stationary regime at large times T, independent of the initial condition. In this statistically steady state, $X_{n,\epsilon}$ is thus fully characterized by its correlation function, conveniently expressed in spectral space. We have*

$$\mathcal{C}_{X_{n,\epsilon}}(\tau) = \int_{\mathbb{R}} \mathrm{e}^{2\,i\pi\omega\tau} 4\pi\omega \frac{T^2}{1+4\pi^2T^2\omega^2} \left[\frac{1}{1+\dfrac{4\pi^2\tau_\eta^2\omega^2}{n-1}}\right]^{n-1} \left(\int_0^\infty \frac{\sin(2\pi\omega h)\,\mathrm{d}h}{h+\epsilon+\sqrt{\epsilon(h+\epsilon)}}\right)\mathrm{d}\omega, \tag{A 20}$$

such that

$$\mathcal{C}_X(\tau) \equiv \lim_{n\to\infty}\lim_{\epsilon\to 0} \mathcal{C}_{X_{n,\epsilon}}(\tau) = \lim_{\epsilon\to 0}\lim_{n\to\infty} \mathcal{C}_{X_{n,\epsilon}}(\tau) \tag{A 21}$$

$$= \int_{\mathbb{R}} \mathrm{e}^{2\,i\pi\omega\tau} 2\pi^2|\omega| \frac{T^2}{1+4\pi^2T^2\omega^2} \exp(-4\pi^2\tau_\eta^2\omega^2)\,\mathrm{d}\omega. \tag{A 22}$$

In particular, we have

$$\mathcal{C}_X(0) = \langle X^2 \rangle = \int_{\mathbb{R}} 2\pi^2 |\omega| \frac{T^2}{1 + 4\pi^2 T^2 \omega^2} \exp(-4\pi^2 \tau_\eta^2 \omega^2)\, \mathrm{d}\omega \tag{A 23}$$

$$\underset{\tau_\eta \to 0}{=} \log\left(\frac{T}{\tau_\eta}\right) + O(1), \tag{A 24}$$

where the $O(1)$ constant is equal to minus one half of the Euler–Mascheroni constant (≈ -0.288), and

$$\lim_{\tau_\eta \to 0} \mathcal{C}_X(\tau) = \mathcal{C}_{X_1}(\tau), \tag{A 25}$$

where X_1 is the single-layer fractional Ornstein–Uhlenbeck process depicted in Proposition A.3.

Concerning the expression of this correlation function in the physical space, it can be written for numerical purposes as

$$\mathcal{C}_X(\tau) = \frac{T}{4\tau_\eta^3} \int_{\mathbb{R}} \mathrm{e}^{-\frac{|\tau - t|}{T}} \left[\tau_\eta - t\mathcal{F}\left(\frac{t}{2\tau_\eta}\right)\right] \mathrm{d}t, \tag{A 26}$$

where the so-called Dawson integral $\mathcal{F}(x) = \mathrm{e}^{-x^2} \int_0^x \mathrm{e}^{y^2}\, \mathrm{d}y$ enters.

Proof. The correlation function $\mathcal{C}_{X_{n,\epsilon}}$ (A 20) corresponds to the successive linear operations made on a white noise $\widetilde{W}(\mathrm{d}t)$: an OU process for a large time scale T, $n-2$ OU processes at the small time scale $\tau_\eta/\sqrt{n-1}$ and a fractional OU process of vanishing Hurst exponent at $\tau_\eta/\sqrt{n-1}$ (and defined in Proposition A.3). Expressions (A 21)–(A 25) follow from this spectral representation. The physical form of $\mathcal{C}_X$ (A 26) is obtained through inverse Fourier transformation of (A 22). □

PROPOSITION A.5 (Concerning the covariance structure of the infinitely differentiable causal MRW u and the corresponding acceleration process). *Assume $\gamma^2 < 1$. The unique statistically stationary solution $u_{n,\epsilon}$ of the set of equations (3.8)–(3.12) converges, as far as the average and variance are concerned, when both $\epsilon \to 0$ and $n \to \infty$ (the limiting procedure commutes) to a zero-average process that we note u.*

Its correlation function reads

$$\mathcal{C}_u(\tau) = \int_{\mathbb{R}} G_T(h+\tau) \mathcal{C}_f(h) \mathrm{e}^{\gamma^2 \mathcal{C}_X(h)}\, \mathrm{d}h \tag{A 27}$$

$$= T\mathrm{e}^{-\frac{|\tau|}{T}} \int_0^{|\tau|} \cosh\left(\frac{h}{T}\right) \mathcal{C}_f(h) \mathrm{e}^{\gamma^2 \mathcal{C}_X(h)}\, \mathrm{d}h + T\cosh\left(\frac{\tau}{T}\right) \int_{|\tau|}^{\infty} \mathrm{e}^{-\frac{h}{T}} \mathcal{C}_f(h) \mathrm{e}^{\gamma^2 \mathcal{C}_X(h)}\, \mathrm{d}h, \tag{A 28}$$

where $\mathcal{C}_X$ corresponds to the correlation function of the infinitely differentiable Gaussian process X depicted in Proposition A.4, and C_f the correlation function of the Gaussian force f entering in the dynamics of u_n (3.8) once the limit $n \to \infty$ has been taken, and given by

$$\mathcal{C}_f(\tau) = \frac{\sigma^2}{T\displaystyle\int_0^{\infty} \mathrm{e}^{-\frac{h}{T}} \mathrm{e}^{-h^2/(4\tau_\eta^2)} \mathrm{e}^{\gamma^2 \mathcal{C}_X(h)}\, \mathrm{d}h} \mathrm{e}^{-\frac{\tau^2}{4\tau_\eta^2}}. \tag{A 29}$$

In the limit of infinite Reynolds number, i.e. as $\tau_\eta/T \to 0$, the correlation function $\mathcal{C}_u$ of u coincides with the one of the single-layered MRW u_1, which was shown in § 3.1 to coincide *itself with the one of the single-layered OU process v_1 (2.1) of variance σ^2, and we have*

$$\lim_{\tau_\eta \to 0} \mathcal{C}_u(\tau) = \mathcal{C}_{u_1}(\tau) = \mathcal{C}_{v_1}(\tau) = \sigma^2 \mathrm{e}^{-\frac{|\tau|}{T}}. \tag{A 30}$$

Rephrased in terms inherited from the phenomenology of turbulence, the asymptotic behaviour of the correlation function (A 30) says that intermittent corrections observed at finite Reynolds numbers (A 27), and governed by the coefficient γ, disappear at infinite Reynolds number. In a similar spirit, these intermittent corrections only affect the dissipative range (i.e. τ of the order and smaller than τ_η), and disappear in the inertial range $\tau_\eta \ll \tau \ll T$.

Going back to finite Reynolds number predictions, i.e. keeping τ_η finite and smaller than T, the expression of the Lagrangian integral time scale T_L is of special interest, and we get

$$T_L = \int_0^\infty \frac{\mathcal{C}_u(\tau)}{\mathcal{C}_u(0)}\, \mathrm{d}\tau = \frac{T^2}{\sigma^2} \int_0^\infty \mathcal{C}_f(h) \mathrm{e}^{\gamma^2 \mathcal{C}_X(h)}\, \mathrm{d}h \underset{\tau_\eta \to 0}{\to} T. \tag{A 31}$$

The corresponding expression for the acceleration correlation function $\mathcal{C}_a$ is then obtained while taking (minus) the second derivatives of $\mathcal{C}_u$ (A 28), and reads

$$\mathcal{C}_a(\tau) = \mathcal{C}_f(\tau) \mathrm{e}^{\gamma^2 \mathcal{C}_X(\tau)} - \frac{1}{T^2} \mathcal{C}_u(\tau). \tag{A 32}$$

Incidentally, the acceleration variance, and its behaviour in the infinite Reynolds number limit (i.e. while looking at the limit $\tau_\eta / T \to 0$), reads

$$\mathcal{C}_a(0) = \langle a^2 \rangle = \mathcal{C}_f(0) \mathrm{e}^{\gamma^2 \mathcal{C}_X(0)} - \frac{\sigma^2}{T^2} \tag{A 33}$$

$$\underset{\tau_\eta / T \to 0}{\sim} \frac{\sigma^2}{\sqrt{\pi} T \tau_\eta}, \tag{A 34}$$

consistent with standard dimensional predictions, with no further intermittent corrections.

Proof. Start with showing the form of the asymptotic correlation function $\mathcal{C}_f$ (A 29) of the force term f, when the number of layers n goes to infinity. Consider first this correlation at a finite n. We have, seeking for the stationary solution of (3.9) and computing its correlation function in the statistically steady regime,

$$\mathcal{C}_{f_{n-1}}(\tau) = \beta_n \int_{\mathbb{R}} \mathrm{e}^{2\mathrm{i}\pi\omega\tau} \left[\frac{\dfrac{\tau_\eta^2}{n-1}}{1 + \dfrac{4\pi^2 \tau_\eta^2 \omega^2}{n-1}} \right]^{n-1} \mathrm{d}\omega.$$

Remark that for all positive x and integers n, by the binomial formula, $(1 + x/n)^n$ is bounded from below by $1 + x$, such that $(1 + 4\pi^2 \tau_\eta^2 \omega^2/(n-1))^{1-n}$ is bounded from above by $(1 + 4\pi^2 \tau_\eta^2 \omega^2)^{-1}$, which is an integrable function. This allows the use of dominated convergence to conclude on the convergence of $\mathcal{C}_{f_{n-1}}$ as $n \to \infty$, once we take for β_n the expression in (3.13). Taking then the limit $n \to \infty$, the inverse Fourier transform of the obtained Gaussian function is computed to arrive at (A 29).

Looking for the stationary solution of u (3.8), once the limit $n \to \infty$ has been taken and keeping in mind that the log-correlated field X is independent of the forcing term f, the velocity correlation function reads $\mathcal{C}_u(\tau) = (g_T \star g_T \star \mathcal{C}_f e^{\gamma^2 \mathcal{C}_X})(\tau)$. This corresponds to the expression provided in (A 27).

Whereas it is straightforward to show the convergence of the correlation function of the process as $\tau_\eta \to 0$ and then $\epsilon \to 0$, the convergence as $\epsilon \to 0$ and only then $\tau_\eta \to 0$, as stated in (A 30), deserves attention. In any case, both orderings of limits give the same convergence towards the one of the OU process (A 30). The full demonstration of this is developed in appendix C, where the convergence of the second-order structure function is studied.

Other assertions of Proposition A.5 follow from the expression of $\mathcal{C}_u$. □

PROPOSITION A.6 (Concerning the scaling of the higher-order structure functions of the infinitely differentiable causal MRW u). *Without loss of generality, consider an infinite number of layers $n \to \infty$, and call u_ϵ the respective process. Define the velocity increment of the process u_ϵ as*

$$\delta_\tau u_\epsilon(t) = u_\epsilon(t+\tau) - u_\epsilon(t). \tag{A 35}$$

Accordingly, define the respective asymptotic structure functions as

$$\mathcal{S}_{u,m}(\tau) = \lim_{\epsilon \to 0} \langle (u_\epsilon(t+\tau) - u_\epsilon(t))^m \rangle . \tag{A 36}$$

As we have seen when presenting the correlation structure of u in proposition A.5, we have, for $\gamma^2 < 1$,

$$\mathcal{S}_{u,2}(\tau) = \lim_{\epsilon \to 0} \mathcal{S}_{u_\epsilon,2}(\tau) = 2\left[\sigma^2 - \mathcal{C}_u(\tau)\right] \underset{\tau_\eta \to 0}{\longrightarrow} 2\sigma^2 \left[1 - e^{-\frac{|\tau|}{T}}\right]. \tag{A 37}$$

With respect to the convergence of the fourth-order structure function $\mathcal{S}_{u_\epsilon,4}$, we have a more subtle behaviour related to the ordering of the limits. We can show that, taking first the limit $\tau_\eta \to 0$ and keeping ϵ finite, $\mathcal{S}_{u_\epsilon,4}$ coincides with the fourth-order structure function of the single-layered MRW u_1 for which scaling properties are listed in § 3.1. More precisely, we can write for $4\gamma^2 < 1$

$$\lim_{\epsilon \to 0} \lim_{\tau_\eta \to 0} \mathcal{S}_{u_\epsilon,4}(\tau) = \mathcal{S}_{u_1,4}(\tau), \tag{A 38}$$

which exhibits an intermittent behaviour (see (3.6), with $q = 2\sigma^2/T$ such that u and u_1 have same variance). In the reverse order of the limits, calculations get intricate, but under an approximation procedure, we obtain the following scaling behaviour

$$\lim_{\tau_\eta \to 0} \lim_{\epsilon \to 0} \mathcal{S}_{u_\epsilon,4}(\tau) = c_{\gamma,4} \mathcal{S}_{u_1,4}(\tau), \tag{A 39}$$

where $c_{\gamma,4}$ is a constant that depends only on the intermittency coefficient γ which can be computed. We can notice that, in this approximation, the ordering of the limits has a consequence only on the value of the multiplicative constant entering in the power laws ((A 38) and (A 39)), whereas the power-law exponent is the same in both cases, and exhibits an intermittent correction.

In a similar way, whereas taking the limit $\tau_\eta \to 0$ and then $\epsilon \to 0$ has no difficulties, we can assert that

$$\lim_{\tau_\eta \to 0} \lim_{\epsilon \to 0} \mathcal{S}_{u_\epsilon,2m}(\tau) = c_{\gamma,2m} \mathcal{S}_{u_1,2m}(\tau), \tag{A 40}$$

showing that u exhibits a log-normal spectrum (take a look at 3.7 with again $q = 2\sigma^2/T$) when the Reynolds number becomes infinite.

We gather all proofs in appendix C.

Appendix B. Scaling properties of the structure functions of the causal multifractal random walk

To set our notations, define various quantities that will enter in following calculations. The velocity increments read

$$\delta_\tau u_{1,\epsilon}(t) = u_{1,\epsilon}(t+\tau) - u_{1,\epsilon}(t) \tag{B 1}$$

$$= \int_{\mathbb{R}} g_{\tau,T}(t-s)\exp(\gamma X_{1,\epsilon}(s) - \gamma^2\langle X_{1,\epsilon}^2\rangle)W(\mathrm{d}s), \tag{B 2}$$

where $g_{\tau,T}$ corresponds to the OU-kernel associated with velocity increments, that is

$$g_{\tau,T}(t) = \sqrt{q}\left[\mathrm{e}^{-\frac{t+\tau}{T}} 1_{t+\tau\ge 0} - \mathrm{e}^{-\frac{t}{T}} 1_{t\ge 0}\right]. \tag{B 3}$$

We obtain

$$\left\langle \left(\delta_\tau u_{1,\epsilon}\right)^2\right\rangle = \int_{\mathbb{R}^2} g_{\tau,T}(t-s_1)g_{\tau,T}(t-s_2)\left\langle \exp(\gamma\left(X_{1,\epsilon}(s_1)+X_{1,\epsilon}(s_2)\right) - 2\gamma^2\langle X_{1,\epsilon}^2\rangle)W(\mathrm{d}s_1)W(\mathrm{d}s_2)\right\rangle \tag{B 4}$$

$$= \int_{\mathbb{R}^2} g_{\tau,T}(t-s_1)g_{\tau,T}(t-s_2)\left\langle \exp(\gamma\left(X_{1,\epsilon}(s_1)+X_{1,\epsilon}(s_2)\right) - 2\gamma^2\langle X_{1,\epsilon}^2\rangle)\right\rangle \times \langle W(\mathrm{d}s_1)W(\mathrm{d}s_2)\rangle \tag{B 5}$$

$$= \int_{\mathbb{R}} g_{\tau,T}^2(t-s)\left\langle \exp(2\gamma X_{1,\epsilon}(s) - 2\gamma^2\langle X_{1,\epsilon}^2\rangle)\right\rangle \mathrm{d}s \tag{B 6}$$

$$= \int_{\mathbb{R}} g_{\tau,T}^2(s)\,\mathrm{d}s, \tag{B 7}$$

where we have used the independence of the fields $X_{1,\epsilon}$ and W, and the fact that $\langle e^x\rangle = \mathrm{e}^{\frac{1}{2}\langle x^2\rangle}$ for any zero-average Gaussian random variable x. It is then easy to see that the result (B 7) would have been the same with the standard Ornstein–Uhlenbeck process v_1 (2.1), which shows that the asymptotic process u_1 has no intermittent corrections up to second order. Performing the remaining integral that enters in (B 7) leads to the result obtained in (3.5).

Concerning the fourth-order structure function, we have in a similar way

$$\left\langle \left(\delta_\tau u_{1,\epsilon}\right)^4\right\rangle = 3\int_{\mathbb{R}^2} g_{\tau,T}^2(t-s_1)g_{\tau,T}^2(t-s_2) \times \left\langle \exp(2\gamma\left(X_{1,\epsilon}(s_1)+X_{1,\epsilon}(s_2)\right) - 4\gamma^2\langle X_{1,\epsilon}^2\rangle)\right\rangle \mathrm{d}s_1\,\mathrm{d}s_2 \tag{B 8}$$

$$= 3\int_{\mathbb{R}^2} g_{\tau,T}^2(t-s_1)g_{\tau,T}^2(t-s_2)\exp(4\gamma^2\mathcal{C}_{X_{1,\epsilon}}(s_1-s_2))\,\mathrm{d}s_1\,\mathrm{d}s_2 \tag{B 9}$$

$$= 6\int_0^\infty \left(g_{\tau,T}^2 \star g_{\tau,T}^2\right)(s)\exp(4\gamma^2\mathcal{C}_{X_{1,\epsilon}}(s))\,\mathrm{d}s, \tag{B 10}$$

where we have used Isserlis' theorem to factorize the four-time correlator of W in terms of products of its correlations, which gives rise to three symmetrical terms of equal contribution, with an appropriate change of variables, and finally exploited the parity of the functions $(g^2_{\tau,T} \star g^2_{\tau,T})$ and $\mathcal{C}_{X_{1,\epsilon}}$. Dominated convergence ensures that

$$\mathcal{S}_{u_1,4}(\tau) = \lim_{\epsilon\to 0}\left\langle\left(\delta_\tau u_{1,\epsilon}\right)^4\right\rangle \tag{B 11}$$

$$= 6\int_0^\infty \left(g^2_{\tau,T} \star g^2_{\tau,T}\right)(s)\exp(4\gamma^2\mathcal{C}_{X_1}(s))\,\mathrm{d}s. \tag{B 12}$$

At this stage, remark that the integral provided in (B 12) makes sense only if the singularity $\sim s^{-4\gamma^2}$ implied by $\exp(4\gamma^2\mathcal{C}_{X_1}(s))$ (as easily seen in (A 17)) is integrable in the vicinity of the origin. This explains the bound on γ required by the existence of the fourth-order structure function, that is

$$4\gamma^2 < 1. \tag{B 13}$$

Compute then the function $(g^2_{\tau,T} \star g^2_{\tau,T})(s)$, namely, for $s \geq 0$ and $\tau \geq 0$,

$$\left(g^2_{\tau,T} \star g^2_{\tau,T}\right)(s) = q^2\mathrm{e}^{-\frac{2s}{T}}\int_{\mathbb{R}} \mathrm{e}^{-\frac{4x}{T}}\left[\mathrm{e}^{-\frac{\tau}{T}}1_{x+\tau\geq 0} - 1_{x\geq 0}\right]^2\left[\mathrm{e}^{-\frac{\tau}{T}}1_{x+\tau+s\geq 0} - 1_{x+s\geq 0}\right]^2\mathrm{d}x, \tag{B 14}$$

which integrand is made up of simple exponentials over intricate domains, and get in an exact fashion (with the help of a symbolic calculation software),

$$\left(g^2_{\tau,T} \star g^2_{\tau,T}\right)(s) = \frac{q^2T}{4}\left[\left(1-\mathrm{e}^{-\frac{\tau}{T}}\right)^3\left(2+\mathrm{e}^{\frac{\tau}{T}}+\mathrm{e}^{2\frac{\tau}{T}}\right)\mathrm{e}^{-2\frac{s}{T}}\right. \tag{B 15}$$

$$\left. +2\left(2\mathrm{e}^{-\frac{\tau}{T}}-1\right)\sinh\left(2\frac{\tau-s}{T}\right)1_{\tau-s\geq 0}\right], \tag{B 16}$$

and inject it into the expression of $\mathcal{S}_{u_1,4}$ (B 12). Observe that the decrease of $\mathcal{S}_{u_1,4}$ as $\tau\to 0$ is governed by the second term $(g^2_{\tau,T} \star g^2_{\tau,T})$ (B 16), since the first term (B 15) implies a decrease towards 0 as τ^3. Thus, only considering the leading contribution entering in (B 16), using $(2\mathrm{e}^{-\tau/T}-1)\approx 1$, we have a good approximation as $\tau\to 0$

$$\mathcal{S}_{u_1,4}(\tau) \approx 3Tq^2\int_0^\tau \sinh\left(\frac{2(\tau-s)}{T}\right)\exp(4\gamma^2\mathcal{C}_{X_1}(s))\,\mathrm{d}s \tag{B 17}$$

$$= 3Tq^2\int_0^1 \sinh\left(\frac{2\tau(1-s)}{T}\right)\exp(4\gamma^2\mathcal{C}_{X_1}(\tau s))\tau\,\mathrm{d}s \tag{B 18}$$

$$\underset{\tau\to 0}{\sim} 6q^2\tau^2\left(\frac{\tau}{T}\right)^{-4\gamma^2}\mathrm{e}^{4\gamma^2 c(0)}\int_0^1 (1-s)\,s^{-4\gamma^2}\,\mathrm{d}s \tag{B 19}$$

$$= \frac{3}{1-6\gamma^2+8\gamma^4}q^2\tau^2\left(\frac{\tau}{T}\right)^{-4\gamma^2}\mathrm{e}^{4\gamma^2 c(0)}, \tag{B 20}$$

where the constant $c(0)$ is explicitly known, and given in (A 18). This entails (3.6).

Let us now generalize former calculations up to any order. We get

$$\left\langle \left(\delta_\tau u_{1,\epsilon}\right)^{2m} \right\rangle = \frac{(2m)!}{2^m m!} \int_{\mathbb{R}^m} \prod_{k=1}^m g^2_{\tau,T}(t-s_k) \left\langle \exp\left(2\gamma \sum_{k=1}^m X_{1,\epsilon}(s_k) - 2m\gamma^2 \langle X^2_{1,\epsilon}\rangle\right)\right\rangle \prod_{k=1}^m \mathrm{d}s_k \quad \text{(B 21)}$$

$$= \frac{(2m)!}{2^m m!} \int_{\mathbb{R}^m} \prod_{k=1}^m g^2_{\tau,T}(t-s_k) \exp\left(4\gamma^2 \sum_{k<p=1}^m \mathcal{C}_{X_{1,\epsilon}}(s_k - s_p)\right) \prod_{k=1}^m \mathrm{d}s_k \quad \text{(B 22)}$$

$$\underset{\epsilon\to 0}{=} \frac{(2m)!}{2^m m!} \int_{\mathbb{R}^m} \prod_{k=1}^m g^2_{\tau,T}(t-s_k) \exp\left(4\gamma^2 \sum_{k<p=1}^m \mathcal{C}_{X_1}(s_k - s_p)\right) \prod_{k=1}^m \mathrm{d}s_k. \quad \text{(B 23)}$$

Once again, the exponential entering in (B 23) gives both the condition of existence on γ, and intermittent corrections. The strongest singularity is encountered along the diagonal, that is when all dummy variables s_k coincide. It is equivalent to say that it is necessary to take

$$2m(m-1)\gamma^2 < 1, \quad \text{(B 24)}$$

to guarantee the existence of the integral given in (B 23). Similarly, it implies an intermittent correction of order $(\tau/T)^{-2m(m-1)\gamma^2}$, as stated in (3.7), which concludes the proofs of § 3.1.

Appendix C. Scaling properties of the structure functions of the infinitely differentiable causal multifractal random walk

To set our notations, we define various quantities that will enter in the following calculations. The velocity increments read

$$\delta_\tau u(t) = u(t+\tau) - u(t) \quad \text{(C 1)}$$

$$= \int_{\mathbb{R}} g_{\tau,T}(t-s) \exp\left(\gamma X(s) - \frac{\gamma^2}{2}\langle X^2\rangle\right) f(s)\,\mathrm{d}s, \quad \text{(C 2)}$$

where $g_{\tau,T}$ corresponds to the OU-kernel associated with velocity increments, that is

$$g_{\tau,T}(t) = \mathrm{e}^{-\frac{t+\tau}{T}} 1_{t+\tau\geq 0} - \mathrm{e}^{-\frac{t}{T}} 1_{t\geq 0}. \quad \text{(C 3)}$$

We obtain

$$\langle(\delta_\tau u)^2\rangle = \int_{\mathbb{R}^2} g_{\tau,T}(t-s_1) g_{\tau,T}(t-s_2) \mathcal{C}_f(s_1-s_2) \times \langle \exp(\gamma\,(X(s_1)+X(s_2)) - \gamma^2\langle X^2\rangle)\rangle\,\mathrm{d}s_1\,\mathrm{d}s_2 \quad \text{(C 4)}$$

$$= \int_{\mathbb{R}^2} g_{\tau,T}(t-s_1) g_{\tau,T}(t-s_2) \mathcal{C}_f(s_1-s_2) \exp(\gamma^2 C_X(s_1-s_2))\,\mathrm{d}s_1\,\mathrm{d}s_2 \quad \text{(C 5)}$$

$$= \int_{\mathbb{R}} \left(g_{\tau,T} \star g_{\tau,T}\right)(s) \mathcal{C}_f(s) \mathrm{e}^{\gamma^2 C_X(s)}\,\mathrm{d}s \quad \text{(C 6)}$$

$$= 2\int_{\mathbb{R}^+} \left(g_{\tau,T} \star g_{\tau,T}\right)(s) \mathcal{C}_f(s) \mathrm{e}^{\gamma^2 C_X(s)}\,\mathrm{d}s, \quad \text{(C 7)}$$

where we have used the independence of the fields X and f, and the fact that $\langle e^x\rangle = \mathrm{e}^{\frac{1}{2}\langle x^2\rangle}$ for any zero-average Gaussian random variable x. This shows that, contrary to the MRW case u_1 (3.5), the asymptotic process u (once the limit $\epsilon \to 0$ has been taken) has an intermittent correction up to second order when τ_η/T is finite. We have, for $\tau \geq 0$ and $s \geq 0$,

$$\left(g_{\tau,T} \star g_{\tau,T}\right)(s) = T\left(\mathrm{e}^{-s/T} - \mathrm{e}^{-\tau/T}\cosh(s/T) + \sinh\left(\frac{s-\tau}{T}\right) 1_{s-\tau\geq 0}\right), \tag{C 8}$$

which shows that once injected in (C 7), we recover in a consistent manner

$$\left\langle (\delta_\tau u)^2 \right\rangle = 2\left(\sigma^2 - C_u(\tau)\right). \tag{C 9}$$

To see the behaviour of the second-order structure function in the (non-commuting) limit $\tau_\eta \to 0$ (i.e. the infinite Reynolds number limit) and then $\tau \to 0$ (i.e. the limit at small scales), regroup terms in (C 8) and obtain, using the definition of $\mathcal{C}_f$ (A 29),

$$\left\langle (\delta_\tau u)^2 \right\rangle = 2\sigma^2\left[1 - \cosh\left(\frac{\tau}{T}\right)\right] + 2\sigma^2 \frac{\displaystyle\int_0^\tau \sinh\left(\frac{\tau - s}{T}\right) \mathrm{e}^{-\frac{s^2}{4\tau_\eta^2}} \mathrm{e}^{\gamma^2 \mathcal{C}_X(s)}\,\mathrm{d}s}{\displaystyle\int_0^\infty \mathrm{e}^{-\frac{s}{T}} \mathrm{e}^{-\frac{s^2}{4\tau_\eta^2}} \mathrm{e}^{\gamma^2 \mathcal{C}_X(s)}\,\mathrm{d}s}. \tag{C 10}$$

Rescale then the dummy variable entering the second term by τ_η and obtain

$$\left\langle (\delta_\tau u)^2 \right\rangle = 2\sigma^2\left[1 - \cosh\left(\frac{\tau}{T}\right)\right] + 2\sigma^2 \frac{\displaystyle\int_0^{\tau/\tau_\eta} \sinh\left(\frac{\tau - s\tau_\eta}{T}\right) \mathrm{e}^{-\frac{s^2}{4}} \exp(\gamma^2 \mathcal{C}_X(s\tau_\eta))\,\mathrm{d}s}{\displaystyle\int_0^\infty \mathrm{e}^{-\frac{s\tau_\eta}{T}} \mathrm{e}^{-\frac{s^2}{4}} \exp(\gamma^2 \mathcal{C}_X(s\tau_\eta))\,\mathrm{d}s}, \tag{C 11}$$

such that we obtain the simple result

$$\lim_{\tau_\eta \to 0} \left\langle (\delta_\tau u)^2 \right\rangle = 2\sigma^2\left[1 - \mathrm{e}^{-\frac{\tau}{T}}\right], \tag{C 12}$$

showing that, up to second-order statistics, the infinitely differentiable causal multifractal walk u coincides with the underlying OU process (2.1) in the infinite Reynolds number limit $\tau_\eta \to 0$.

Concerning the fourth-order structure function, we have in a similar way

$$\left\langle (\delta_\tau u)^4 \right\rangle = 3\int_{\mathbb{R}^4} \prod_{k=1}^4 g_{\tau,T}(t - s_k) \left\langle \exp\left(\gamma \sum_{k=1}^4 X(s_k) - 2\gamma^2 \langle X^2 \rangle\right)\right\rangle \\ \times \mathcal{C}_f(s_1 - s_2)\mathcal{C}_f(s_3 - s_4) \prod_{k=1}^4 \mathrm{d}s_k \tag{C 13}$$

$$= 3\int_{\mathbb{R}^4} \prod_{k=1}^4 g_{\tau,T}(s_k) \exp\left(\gamma^2 \sum_{k<p=1}^4 \mathcal{C}_X(s_k - s_p)\right) \\ \times \mathcal{C}_f(s_1 - s_2)\mathcal{C}_f(s_3 - s_4) \prod_{k=1}^4 \mathrm{d}s_k \tag{C 14}$$

$$= 3\int_{\mathbb{R}^4} g_{\tau,T}(s)g_{\tau,T}(s-h_1)g_{\tau,T}(s-h_2)g_{\tau,T}(s-h_3) \tag{C 15}$$

$$\times \exp(\gamma^2 (\mathcal{C}_X(h_1)+\mathcal{C}_X(h_2)+\mathcal{C}_X(h_3)+\mathcal{C}_X(h_1-h_2)$$
$$+\mathcal{C}_X(h_1-h_3)+\mathcal{C}_X(h_2-h_3))) \tag{C 16}$$

$$\times \mathcal{C}_f(h_1)\mathcal{C}_f(h_3-h_2)\,\mathrm{d}s\prod_{k=1}^{3}\mathrm{d}h_k \tag{C 17}$$

$$= 3\int_{\mathbb{R}^3} G_{\tau,T}(h_1,h_2,h_3)\mathcal{C}_f(h_1)\mathcal{C}_f(h_2-h_3)$$
$$\times \exp\left(\gamma^2\left(\sum_{k=1}^{3}\mathcal{C}_X(h_k)+\sum_{k<l,1}^{3}\mathcal{C}_X(h_k-h_l)\right)\right)\prod_{k=1}^{3}\mathrm{d}h_k, \tag{C 18}$$

where we have noted

$$G_{\tau,T}(h_1,h_2,h_3) = \int_{\mathbb{R}} g_{\tau,T}(s)g_{\tau,T}(s+h_1)g_{\tau,T}(s+h_2)g_{\tau,T}(s+h_3)\,\mathrm{d}s. \tag{C 19}$$

The exact expression of the function $G_{\tau,T}$ (C 19) could be obtained using a symbolic calculation software, although it is intricate. Instead, we will do an approximate calculation, based on an ansatz for the correlation function $\mathcal{C}_X$ entering in the expression of the moment of velocity increments (C 18). We get then an equivalent at infinite Reynolds number (i.e. $\tau_\eta \to 0$), from which we deduce the scaling behaviour as τ goes to zero.

As we have seen, the correlation function $\mathcal{C}_X(\tau)$ of X (A 22) has several obvious limiting behaviours. First, it goes to zero at large arguments $\tau \gg T$. Secondly, as $\tau_\eta \to 0$, its value at the origin blows up logarithmically with τ_η (A 24), and in the same limit, pointwise, for strictly positive arguments $\tau > 0$, it behaves logarithmically with τ as $\tau \to 0$. A simple ansatz for $\mathcal{C}_X(\tau)$ consistent with these limiting behaviours could be written in an approximate and simple way as

$$\mathcal{C}_X(\tau) \approx \frac{1}{2}\log\frac{T^2}{\tau_\eta^2+\tau^2}1_{|\tau|\le T} + \mathrm{d}_{\tau_\eta}(\tau), \tag{C 20}$$

where $\mathrm{d}_{\tau_\eta}(\tau)$ is a bounded function of τ and τ_η, that goes to zero at large arguments. Furthermore, we know that $\mathrm{d}_{\tau_\eta}(0) \to d(0)$ coincides with minus one half the Euler–Mascheroni constant (i.e. ≈ -0.288) as $\tau_\eta \to 0$ (A 24). Henceforth, calculations will not be performed in a rigorous way since the ansatz (C 20) in only an approximate, although realistic, form of $\mathcal{C}_X$.

Find now the pointwise behaviour of the correlation function C_f of f (A 29). We have, looking for an equivalent of the multiplicative factor entering in (A 29), using the ansatz proposed in (C 20),

$$\frac{T(T/\tau_\eta)^{\gamma^2}\mathrm{e}^{\gamma^2 d(0)}g(\gamma)}{\sigma^2}\mathcal{C}_f(\tau) \underset{\tau_\eta\to 0}{\sim} \frac{1}{\sqrt{4\pi\tau_\eta^2}}\mathrm{e}^{-\frac{\tau^2}{4\tau_\eta^2}}, \tag{C 21}$$

where

$$g(\gamma) = \frac{1}{\sqrt{4\pi}}\int_0^\infty \mathrm{e}^{-h^2/4}\frac{1}{(1+h^2)^{\gamma^2}}\,\mathrm{d}h. \tag{C 22}$$

From the equivalent derived in (C 21), we can see that $\mathcal{C}_f$, properly weighted, will participate to the fourth-order moment of increments (C 18) similarly to a distributional Dirac function, and will greatly simplify its expression. Checking the realism of the ansatz (C 21) on the second-order structure function (C 6) we obtain $\langle(\delta_\tau u)^2\rangle \sim (\sigma^2/Tg(\gamma))(g_{\tau,T} \star g_{\tau,T})(0) = (\sigma^2/g(\gamma))(1-\mathrm{e}^{-\tau/T})$ as $\tau_\eta \to 0$. We can see that the approach based on the ansatz (C 20) introduces an error compared with the exact result given in (C 12): instead of the exact factor 2 entering in (C 12), we find the factor $1/g(\gamma) \approx 2.1388$ once is used the empirical intermittency coefficient given in (3.25), corresponding thus to an overestimation of order $1/(2g(\gamma)) \approx 7\,\%$ of the multiplicative constant, the remaining power-law dependence on τ being correct.

Having justified the good performance of this approximate procedure, we inject then (C 21) into (C 18), and use the limiting behaviour of $\mathcal{C}_X$ as $\tau_\eta \to 0$ (A 25), and get in a heuristic fashion the following expression

$$\left\langle(\delta_\tau u)^4\right\rangle \underset{\tau_\eta\to 0}{\sim} 6\frac{\sigma^4}{g^2(\gamma)T^2}\int_0^\infty G_{\tau,T}(0,h,h)\exp(4\gamma^2\mathcal{C}_{X_1}(h))\,\mathrm{d}h. \tag{C 23}$$

Noticing that $G_{\tau,T}(0,h,h) = (g^2_{\tau,T} \star g^2_{\tau,T})(h)$, we recover the fourth-order structure function of the MRW process (B 12) using $q = 2\sigma^2/T$ in (B 3) (to make sure that we are comparing two processes of same variance σ^2) up to a multiplicative factor such that

$$\left\langle(\delta_\tau u)^4\right\rangle \underset{\tau_\eta\to 0}{\sim} \frac{1}{4g^2(\gamma)}\left\langle(\delta_\tau u_1)^4\right\rangle. \tag{C 24}$$

The numerical value of this factor is $1/4g^2(\gamma) \approx 1.1436$ working with the empirical value for γ (3.25), saying that $\langle(\delta_\tau u)^4\rangle$ is very similar to $\langle(\delta_\tau u_1)^4\rangle$ at large Reynolds number, in particular its (intermittent) scaling behaviour with τ (see (B 20)).

Let us end this appendix by computing, under the very same approximation based on (C 20), higher-order structure functions. We have

$$\left\langle(\delta_\tau u)^{2m}\right\rangle \tag{C 25}$$

$$= \frac{(2m)!}{2^m m!}\int_{\mathbb{R}^{2m}}\prod_{k=1}^{2m} g_{\tau,T}(t-s_k)\left\langle \exp\left(\gamma\sum_{k=1}^{2m} X(s_k) - m\gamma^2\langle X^2\rangle\right)\right\rangle \prod_{k=1}^{m}$$

$$\times\, \mathcal{C}_f(s_{2k-1}-s_{2k})\prod_{k=1}^{2m}\mathrm{d}s_k \tag{C 26}$$

$$= \frac{(2m)!}{2^m m!}\int_{\mathbb{R}^{2m}}\prod_{k=1}^{2m} g_{\tau,T}(t-s_k)\exp\left(\gamma^2\sum_{k<l,1}^{2m}\mathcal{C}_X(s_k-s_l)\right)\prod_{k=1}^{m}\mathcal{C}_f(s_{2k-1}-s_{2k})\prod_{k=1}^{2m}\mathrm{d}s_k \tag{C 27}$$

$$\underset{\tau_\eta\to 0}{\sim} \frac{(2m)!}{2^m m!}\left(\frac{\sigma^2}{g(\gamma)T}\right)^m\int_{\mathbb{R}^m}\prod_{k=1}^{m} g^2_{\tau,T}(t-s_k)\exp\left(\gamma^2\sum_{k<l,1}^{m}\mathcal{C}_{X_1}(s_k-s_l)\right)\prod_{k=1}^{m}\mathrm{d}s_k, \tag{C 28}$$

showing that

$$\left\langle(\delta_\tau u)^{2m}\right\rangle \underset{\tau_\eta\to 0}{\sim} \frac{1}{2^m g^m(\gamma)}\left\langle(\delta_\tau u_1)^{2m}\right\rangle, \tag{C 29}$$

which entails (A 40).

REFERENCES

ARNEODO, A., BACRY, E. & MUZY, J.-F. 1998 Random cascades on wavelet dyadic tree. *J. Math. Phys.* **39**, 4142–4164.

ARNEODO, A., BENZI, R., BERG, J., BIFERALE, L., BODENSCHATZ, E., BUSSE, A., CALZAVARINI, E., CASTAING, B., CENCINI, M., CHEVILLARD, L., *et al.* 2008 Universal intermittent properties of particle trajectories in highly turbulent flows. *Phys. Rev. Lett.* **100**, 254504.

ARRATIA, A., CABANA, A. & CABANA, E. M. 2014 Modeling stationary data by a class of generalized Ornstein–Uhlenbeck processes: the Gaussian case. In *International Symposium on Intelligent Data Analysis*, pp. 13–24. Springer.

BACRY, E., DELOUR, J. & MUZY, J.-F. 2001 Multifractal random walk. *Phys. Rev.* E **64**, 026103.

BACRY, E. & MUZY, J.-F. 2003 Log-infinitely divisible multifractal processes. *Commun. Math. Phys.* **236** (3), 449–475.

BATCHELOR, G. K. 1951 Pressure fluctuations in isotropic turbulence. In *Mathematical Proceedings of the Cambridge Philosophical Society*, vol. 47, pp. 359–374. Cambridge University Press.

BEC, J., BIFERALE, L., BOFFETTA, G., CELANI, A., CENCINI, M., LANOTTE, A., MUSACCHIO, S. & TOSCHI, F. 2006 Acceleration statistics of heavy particles in turbulence. *J. Fluid Mech.* **550**, 349–358.

BEC, J., BIFERALE, L., CENCINI, M., LANOTTE, A. S. & TOSCHI, F. 2011 Spatial and velocity statistics of inertial particles in turbulent flows. *J. Phys.: Conf. Ser.* **333**, 012003.

BECK, C. 2003 Lagrangian acceleration statistics in turbulent flows. *Europhys. Lett.* **64** (2), 151–157.

BENTKAMP, L., LALESCU, C. C. & WILCZEK, M. 2019 Persistent accelerations disentangle Lagrangian turbulence. *Nat. Commun.* **10**, 1–8

BENZI, R., BIFERALE, L., CRISANTI, A., PALADIN, G., VERGASSOLA, M. & VULPIANI, A. 1993 A random process for the construction of multiaffine fields. *Physica* D **65**, 352–358.

BENZI, R., BIFERALE, L., FISHER, R., LAMB, D. Q. & TOSCHI, F. 2010 Inertial range Eulerian and Lagrangian statistics from numerical simulations of isotropic turbulence. *J. Fluid Mech.* **653**, 221–244.

BIFERALE, L., BOFFETTA, G., CELANI, A., DEVENISH, B. J., LANOTTE, A. & TOSCHI, F. 2004 Multifractal statistics of Lagrangian velocity and acceleration in turbulence. *Phys. Rev. Lett.* **93** (6), 064502.

BORGAS, M. S. 1993 The multifractal Lagrangian nature of turbulence. *Phil. Trans. R. Soc. Lond.* A **342**, 379–411.

BORGAS, M. S. & SAWFORD, B. L. 1994 Stochastic equations with multifractal random increments for modeling turbulent dispersion. *Phys. Fluids* **6** (2), 618–633.

BOS, W. J. T., CHEVILLARD, L., SCOTT, J. F. & RUBINSTEIN, R. 2012 Reynolds number effect on the velocity increment skewness in isotropic turbulence. *Phys. Fluids* **24** (1), 015108.

BUARIA, D., PUMIR, A., BODENSCHATZ, E. & YEUNG, P. K. 2019 Extreme velocity gradients in turbulent flows. *New J. Phys.* **21** (4), 043004.

CASTAING, B., GAGNE, Y. & HOPFINGER, E. 1990 Velocity probability density functions of high Reynolds number turbulence. *Physica* D **46**, 177–200.

CHEVILLARD, L. 2017 Regularized fractional ornstein-uhlenbeck processes and their relevance to the modeling of fluid turbulence. *Phys. Rev.* E **96** (3), 033111.

CHEVILLARD, L., CASTAING, B., ARNEODO, A., LÉVÊQUE, E., PINTON, J.-F. & ROUX, S. 2012 A phenomenological theory of Eulerian and Lagrangian velocity fluctuations in turbulent flows. *C. R. Phys.* **13**, 899–928.

CHEVILLARD, L., CASTAING, B. & LÉVÊQUE, E. 2005 On the rapid increase of intermittency in the near-dissipation range of fully developed turbulence. *Eur. Phys. J.* B **45**, 561–567.

CHEVILLARD, L., CASTAING, B., LÉVÊQUE, E. & ARNEODO, A. 2006 Unified multifractal description of velocity increments statistics in turbulence: intermittency and skewness. *Physica* D **218**, 77–82.

CHEVILLARD, L., GARBAN, C., RHODES, R. & VARGAS, V. 2019 On a skewed and multifractal unidimensional random field, as a probabilistic representation of Kolmogorov's views on turbulence. *Ann. Henri Poincaré* **20** (11), 3693–3741.

CHEVILLARD, L., ROUX, S. G., LÉVÊQUE, E., MORDANT, N., PINTON, J.-F. & ARNEODO, A. 2003 Lagrangian velocity statistics in turbulent flows: effects of dissipation. *Phys. Rev. Lett.* **91**, 214502.

DUBRULLE, B. 2019 Beyond Kolmogorov cascades. *J. Fluid Mech.* **867**, P1.
FRIEDRICH, R. 2003 Statistics of Lagrangian velocities in turbulent flows. *Phys. Rev. Lett.* **90** (8), 084501.
FRISCH, U. 1995 *Turbulence, The Legacy of A.N. Kolmogorov*. Cambridge University Press.
HILL, R. J. 2002 Scaling of acceleration in locally isotropic turbulence. *J. Fluid Mech.* **452**, 361–370.
HUCK, P. D., MACHICOANE, N. & VOLK, R. 2019 Lagrangian acceleration timescales in anisotropic turbulence. *Phys. Rev. Fluids* **4** (6), 064606.
ISHIHARA, T., KANEDA, Y., YOKOKAWA, M., ITAKURA, K. & UNO, A. 2007 Small-scale statistics in high-resolution direct numerical simulation of turbulence: Reynolds number dependence of one-point velocity gradient statistics. *J. Fluid Mech.* **592**, 335–366.
LA PORTA, A., VOTH, G. A., CRAWFORD, A. M., ALEXANDER, J. & BODENSCHATZ, E. 2001 Fluid particle accelerations in fully developed turbulence. *Nature* **409**, 1017–1019.
LAMORGESE, A. G., POPE, S. B., YEUNG, P. K. & SAWFORD, B. L. 2007 A conditionally cubic-Gaussian stochastic Lagrangian model for acceleration in isotropic turbulence. *J. Fluid Mech.* **582**, 423–448.
LI, Y., PERLMAN, E., WAN, M., YANG, Y., BURNS, R., MENEVEAU, C., BURNS, R., CHEN, S., SZALAY, A. & EYINK, G. 2008 A public turbulence database cluster and applications to study Lagrangian evolution of velocity increments in turbulence. *J. Turbul.* **9**, 31.
MENEVEAU, C. 1996 On the transition between viscous and inertial-range scaling of turbulence structure functions. *Phys. Rev.* E **54**, 3657–3663.
MENEVEAU, C. & SREENIVASAN, K. R. 1987 Simple multifractal cascade model for fully developed turbulence. *Phys. Rev. Lett.* **59**, 1424–1427.
MINIER, J.-P., CHIBBARO, S. & POPE, S. B. 2014 Guidelines for the formulation of Lagrangian stochastic models for particle simulations of single-phase and dispersed two-phase turbulent flows. *Phys. Fluids* **26** (11), 113303.
MONIN, A. S. & YAGLOM, A. M. 1971 *Statistical Fluid Mechanics*, vol. 1 and 2. MIT.
MORDANT, N., DELOUR, J., LÉVEQUE, E., ARNÉODO, A. & PINTON, J.-F. 2002 Long time correlations in Lagrangian dynamics: a key to intermittency in turbulence. *Phys. Rev. Lett.* **89** (25), 254502.
MORDANT, N., DELOUR, J., LÉVÊQUE, E., MICHEL, O., ARNEODO, A. & PINTON, J.-F. 2003 Lagrangian velocity fluctuations in fully developed turbulence: scaling, intermittency and dynamics. *J. Stat. Phys.* **112**, 701–717.
MORDANT, N., METZ, P., MICHEL, O. & PINTON, J.-F. 2001 Measurement of Lagrangian velocity in fully developed turbulence. *Phys. Rev. Lett.* **87** (21), 214501.
NELKIN, M. 1990 Multifractal scaling of velocity derivatives in turbulence. *Phys. Rev.* A **42** (12), 7226–7229.
NUALART, D. 2000 *The Malliavin Calculus and Related Topics*. Springer.
PALADIN, G. & VULPIANI, A. 1987 Degrees of freedom of turbulence. *Phys. Rev.* A **35**, 1971–1973.
PAPOULIS, A. 1991 *Probability, Random Variables and Stochastic Processes*, 3rd edn. McGraw-Hill International Editions.
PEREIRA, R. M., GARBAN, C. & CHEVILLARD, L. 2016 A dissipative random velocity field for fully developed fluid turbulence. *J. Fluid Mech.* **794**, 369–408.
PEREIRA, R. M., MORICONI, L. & CHEVILLARD, L. 2018 A multifractal model for the velocity gradient dynamics in turbulent flows. *J. Fluid Mech.* **839**, 430–467.
PINTON, J.-F. & SAWFORD, B. L. 2012 A Lagrangian view of turbulent dispersion and mixing. In *Ten Chapters in Turbulence* (ed. P. A. Davidson, Y. Kaneda & K. R. Sreenivasan), pp. 132–175. Cambridge University Press.
POPE, S. B. 1990 Lagrangian microscales in turbulence. *Phil. Trans. R. Soc. Lond.* A **333** (1631), 309–319.
POPE, S. B. 2002 A stochastic Lagrangian model for acceleration in turbulent flows. *Phys. Fluids* **14** (7), 2360–2375.
POPE, S. B. & CHEN, Y. L. 1990 The velocity-dissipation probability density function model for turbulent flows. *Phys. Fluids* A **2** (8), 1437–1449.
REYNOLDS, A. M. 2003 Superstatistical mechanics of tracer-particle motions in turbulence. *Phys. Rev. Lett.* **91** (8), 084503.
REYNOLDS, A. M., MORDANT, N., CRAWFORD, A. M. & BODENSCHATZ, E. 2005 On the distribution of Lagrangian accelerations in turbulent flows. *New J. Phys.* **7** (1), 58.

RHODES, R. & VARGAS, V. 2014 Gaussian multiplicative chaos and applications: a review. *Probab. Surveys* **11**, 315–392.

ROBERT, R. & VARGAS, V. 2010 Gaussian multiplicative chaos revisited. *Ann. Probab.* **38** (2), 605–631.

SAWFORD, B. L. 1991 Reynolds number effects in Lagrangian stochastic models of turbulent dispersion. *Phys. Fluids* A **3** (6), 1577–1586.

SAWFORD, B. L., YEUNG, P. K., BORGAS, M. S., VEDULA, P., LA PORTA, A., CRAWFORD, A. M. & BODENSCHATZ, E. 2003 Conditional and unconditional acceleration statistics in turbulence. *Phys. Fluids* **15** (11), 3478–3489.

SCHMITT, F. & MARSAN, D. 2001 Stochastic equations generating continuous multiplicative cascades. *Eur. Phys. J.* B **20** (1), 3–6.

TENNEKES, H. & LUMLEY, J. L. 1972 *A First Course in Turbulence*. MIT.

TOSCHI, F. & BODENSCHATZ, E. 2009 Lagrangian properties of particles in turbulence. *Ann. Rev. Fluid Mech.* **41**, 375–404.

VOTH, G. A., SATYANARAYAN, K. & BODENSCHATZ, E. 1998 Lagrangian acceleration measurements at large Reynolds numbers. *Phys. Fluids* **10**, 2268–2280.

WILSON, J. D. & SAWFORD, B. L. 1996 Review of Lagrangian stochastic models for trajectories in the turbulent atmosphere. *Boundary-Layer Meteorol.* **78**, 191–120.

YAKHOT, V. & SREENIVASAN, K. R. 2005 Anomalous scaling of structure functions and dynamic constraints on turbulence simulations. *J. Stat. Phys.* **121** (5-6), 823–841.

YEUNG, P. K. & POPE, S. B. 1989 Lagrangian statistics from direct numerical simulations of isotropic turbulence. *J. Fluid Mech.* **207**, 531–586.

YEUNG, P. K., POPE, S. B., KURTH, E. A. & LAMORGESE, A. G. 2007 Lagrangian conditional statistics, acceleration and local relative motion in numerically simulated isotropic turbulence. *J. Fluid Mech.* **582**, 399–422.

YEUNG, P. K., POPE, S. B., LAMORGESE, A. G. & DONZIS, D. A. 2006 Acceleration and dissipation statistics of numerically simulated isotropic turbulence. *Phys. Fluids* **18** (6), 065103.

YU, H., KANOV, K., PERLMAN, E., GRAHAM, J., FREDERIX, E., BURNS, R., SZALAY, A., EYINK, G. & MENEVEAU, C. 2012 Studying Lagrangian dynamics of turbulence using on-demand fluid particle tracking in a public turbulence database. *J. Turbul.* **13**, N12.